

Non-Gaussianities in generalized non-local R^2 -like inflation

Alexey S. Koshelev,^a K. Sravan Kumar,^b Alexei A. Starobinsky^{c,d}

^a *Departamento de Física, Centro de Matemática e Aplicações (CMA-UBI), Universidade da Beira Interior, 6200 Covilhã, Portugal*

^b *Department of Physics, Tokyo Institute of Technology, 2-12-1 Ookayama, Meguro-ku, Tokyo 152-8551, Japan*

^c *L. D. Landau Institute for Theoretical Physics RAS, Chernogolovka, Moscow region 142432, Russian Federation*

^d *Kazan Federal University, Kazan 420008, Republic of Tatarstan, Russian Federation*

E-mail: alexey@ubi.pt, sravan.k.aa@m.titech.ac.jp, alstar@landau.ac.ru

ABSTRACT: In [1], a most general higher curvature non-local gravity action admitting R^2 -like inflationary solution predicting scalar spectral index $n_s(N) \approx 1 - \frac{2}{N}$, where N is the number of e-folds before the end of inflation, $N \gg 1$, any value of the tensor-to-scalar ratio $r(N) < 0.036$ and tensor tilt $n_t(N)$ violating the $r = -8n_t$ condition was obtained. In this paper, we compute scalar primordial non-Gaussianities (PNGs) in this theory and effectively demonstrate that higher curvature non-local terms lead to new shapes of reduced bispectrum $f_{\text{NL}}(k_1, k_2, k_3)$ mimicking several classes of scalar field models of inflation known in the literature. We obtain $|f_{\text{NL}}| \sim O(1-10)$ in the equilateral, orthogonal, and squeezed limits and the running of PNGs measured by the quantity $|\frac{d \ln f_{\text{NL}}}{d \ln k}| \lesssim 1$. We project these results in the scope of future CMB, Large Scale Structure observations to probe the nature of quantum gravity. Furthermore, we demonstrate that R^2 -like inflation in non-local modification of gravity brings a paradigm shift in our understanding of early Universe cosmology through non-trivial predictions which go beyond the current status of effective field theories (EFTs) of single field, quasi-single field and multiple field inflation. In summary, through our generalized non-local R^2 -like inflation, we obtain for the first time a robust geometric framework of inflation that can explain any detection of observable quantities related to scalar PNGs.

KEYWORDS: Models of Quantum Gravity, Cosmology of Theories beyond the SM

Contents

1	Introduction	1
2	Summary of our results	3
3	Generalized non-local R^2-like inflation	5
4	PNGs and their running in generalized non-local R^2-like inflation	8
4.1	Shape of $f_{\text{NL}}(k_1, k_2, k_3)$ and its running n_{NG}	11
4.2	Quantum fluctuations and the bi-spectrum	14
5	Numerical illustration for shapes of f_{NL} and their running $n_{f_{\text{NL}}}$	14
5.1	The case with only non-local quadratic term in curvature scalar: $\lambda_c = 0$	15
5.2	New shapes and running of PNGs with all the terms in (3.2)	15
6	Distinguishing generalized non-local R^2-like inflation against EFT of scalar field inflation	16
7	Outlook	21
A	Computation of non-Gaussianities	22
B	On violation of Maldacena consistency relation in non-local gravity	24

1 Introduction

Present CMB observations strongly support the R^2 (or Starobinsky) inflation where quasi-de Sitter (dS) expansion is a result of a phase when Ricci scalar R being an eigenmode of d'Alembertian operator [2], see also [3–7]. In a recent paper of the authors [1], a most general higher curvature non-local gravity action that leads to R^2 -like inflationary phase with a scalaron and a massless graviton degrees of freedom was obtained. It is motivated from several quantum gravity frameworks, especially the proposition that an action of quantum gravity should be an extension of general relativity (GR) with all possible curvature invariant terms one can write. The generalized non-local R^2 -like inflation developed in [1] was shown to be compatible with the observed scalar spectral index $n_s = 0.9649 \pm 0.0042$ at 68% CL [8] and any value of the tensor-to-scalar ratio consistent with the latest upper bound $r < 0.036$ [9]. It also admits both positive and negative values of the tensor spectral index n_t and violation of the single field tensor consistency relation $r = -8n_t$. Furthermore, it was found that the generalized non-local R^2 -like inflation [1] does not fall into any categories of so-called effective field theory of single field inflation (EFT-SI) [10, 11] since the framework

of gravity is non-local in nature and does not introduce any non-trivial sound speeds for the perturbed degrees of freedom. In this paper, we compute 3-point scalar correlations or the scalar Primordial Non-Gaussianities (PNGs) of generalized non-local R^2 -like inflation and confront our results against the well-known shapes of non-Gaussianities [12] in terms of the reduced bispectrum f_{NL} [13] constrained from the latest CMB data as follows [14]¹

$$f_{\text{NL}}^{\text{sq}} = -0.9 \pm 5.1, \quad f_{\text{NL}}^{\text{equiv}} = -26 \pm 47, \quad f_{\text{NL}}^{\text{ortho}} = -38 \pm 24 \text{ at } 68\% \text{ CL}. \quad (1.1)$$

PNGs in the case of standard single field (canonical scalar field) inflation are very small to be detectable (i.e., $f_{\text{NL}} \sim O(10^{-2})$), but models based on non-canonical scalar(s) (also generalized scalar-tensor theories like Horndeski [15]) and constructions with non adiabatic vacuum (non-Bunch-Davies) initial conditions are known to give large PNGs with respect to equilateral ($f_{\text{NL}}^{\text{eq}}$) and orthogonal ($f_{\text{NL}}^{\text{orth}}$) bispectrum shapes, whereas squeezed bispectrum ($f_{\text{NL}}^{\text{sq}}$) shape is understood to be the feature of multiple scalar fields or non-slow-roll inflation or non-trivial initial conditions for quantum states [12, 16, 17]. There has been plethora of inflationary models developed in the context of effective field theories (EFTs) to address different shapes of PNGs [10, 18–22]. Furthermore, recent developments of quasi-single field inflation present new signatures for PNGs due to the presence of heavy fields coupled to the inflaton [23, 24]. In summary, any detection of PNGs, i.e., $f_{\text{NL}} \sim O(1 - 10)$ with the present constraints [18] is majorly understood to be the only feature of physics beyond the standard canonical scalar field inflation that are mentioned above. However, in this paper a new understanding of the shapes of PNGs emerges in the context of analytic non-local gravity where the nature of propagating degrees of freedom significantly deviate from the standard effective field theories (EFTs) of inflation in which “locality” is preserved, but the dispersion relations are modified due to time dependent parameters multiplying the spatial derivative terms.

Our framework of study is how higher curvature non-local gravity affects the shapes of $f_{\text{NL}}(k_1, k_2, k_3)$. We ultimately obtain a clear conclusion that squeezed, equilateral and orthogonal templates can be well explained by geometrical modifications of gravity mimicking several classes of scalar-tensor theories. We also study the scale dependent nature of bi-spectrum in our theory of inflation. We envisage all the possible observational features of our geometric non-local R^2 -like inflation in the context of 3-point scalar correlations and provide a detailed discussion to distinguish our framework with large class of EFTs of inflation involving scalar fields.

The paper is organized as follows. In **Sec. 2** we provide a concise summary of results obtained in this paper on PNGs in generalized non-local R^2 -like inflation. In **Sec. 3** we review briefly the generalized non-local gravity action obtained in [1]. In **Sec. 4** and **Sec. 5** we compute PNGs of generalized non-local R^2 -like inflation and discuss several shapes of PNGs which arise from different dimensionless free-parameter values. We compute the running of PNGs defined by the Non-Gaussianity spectral index $n_{\text{NG}} = \frac{d \ln f_{\text{NL}}}{d \ln k}$ and provide details of reconstructing the formfactors in the theory through future cosmological

¹In the literature “squeezed” shape $f_{\text{NL}}^{\text{sq}}$ is most often called as “local” shape [12, 14], but we stick to the definition of “squeezed” shape [13] just in order not to confuse with the meaning of “locality” in this paper.

observations with the ultimate aim to probe the scale of non-locality. We quantitatively elucidate in detail the scale dependent nature of reduced bispectrum in this theory. In **Sec. 6** we provide an extensive discussion of distinguishing the features of generalized non-local R^2 -like inflation against several class of EFTs of inflation involving single and multiple scalar fields. We show how generalized non-local R^2 -like inflation reshapes our understanding of early Universe cosmology. In **Sec. 7** we discuss further studies which are possible to perform beyond the scope of this paper. In **Appendix A** we provide additional details for the computation of PNGs performed in Sec. 4 and Sec. 5. In **Appendix B** we provide a heuristic explanation for violation of the Maldacena consistency relation in non-local gravity despite having slow-roll and single field behaviour during inflation and the adiabatic vacuum initial conditions.

Notations: In this paper, our metric signature is $(-, +, +, +)$. We use overdot and $'$ denotes derivative with respect to cosmic time (t) and conformal time (τ) respectively, $\dagger, \ddagger, \ddagger\ddagger$ for first, second and third derivative with respect to the argument. We use overbar to denote background quantities for flat Friedmann-Lemaître-Robertson-Walker (FLRW) spacetime, 4-dimensional indices are labelled by small Greek letters and three dimensional quantities are denoted by $i, j = 1, 2, 3$. We also set $\hbar = c = 1$ and $M_p = 1/\sqrt{8\pi G}$ is the reduced Planck mass. Everywhere we perform the computations in the leading order in slow-roll parameters ($\epsilon \sim \frac{1}{N}$ approximation). The subscript “_{ds}” denotes the quantities in the quasi-dS approximation.

2 Summary of our results

Primordial Non-Gaussianities (PNGs) are an important probe to understand the nature of self-interactions of primordial fields during inflation. In this paper, we studied the scalar PNGs emerging from generalized non-local R^2 -like inflation which is developed in [1] from the quest of finding a most general quantum gravity action compatible with the so far observed physics of early Universe cosmology. Our results show that it is possible to generate interesting shapes of scalar PNGs in a geometric framework of inflation (i.e, extension of GR with higher derivative and higher curvature terms). The novelty of our study is that we obtain several interesting shapes of PNGs by just changing the dimensionless finite number of free parameters of the generalized non-local R^2 -like inflation [1]. Most importantly, the predictions of PNGs we report in this paper do not affect the observables of scalar and tensor power spectrum such as

$$\left\{ n_s, \frac{dn_s}{d \ln k}, r, n_t, \frac{dn_t}{d \ln k}, \frac{d^2 n_t}{d^2 \ln k} \right\} \quad (2.1)$$

which is often the case in the several class of inflationary models based on the scalar fields [25] (see Sec. 6 for an extensive discussion). The generalized non-local gravity action [1] given in (3.2) describes the most general gravity theory that leads to R^2 -like inflation. The action (3.2) contains analytic infinite derivative (non-local) terms quadratic and cubic in scalar curvature R and non-local terms involving Weyl tensor square and Weyl tensor cube etc. First, we prove that in the leading order of the slow-roll approximation (but

accounting for all corrections from infinite derivative terms), the scalar PNGs in this theory are generated only from the terms that do not contain Weyl tensor. The terms involving Weyl tensor are relevant for tensor PNGs which are the subject of future investigation [26]. Secondly, we compute scalar PNGs in the theory and discover various shapes which appear as a result of changing the (finite) parameter space of the theory. Most importantly, we obtain new shapes of PNGs which are due to the non-local terms cubic in scalar curvature that is a new revelation in comparison with the earlier constructions of non-local R^2 -like inflation with quadratic curvature terms² [27]. Furthermore, we compute running of PNGs in this theory which turned out to be most interesting aspect of non-local theory in the scope of future cosmological observations.

The central message of our study is that large PNGs³ can appear in a purely geometric modification of gravity in a very non-trivial way breaking all the known theorems of EFT of inflation which states [12, 16] that large scalar PNGs can only be generated if one goes beyond the following conditions:

- canonical single field inflation with the speed of sound $c_s = 1$;
- standard slow-roll;
- adiabatic vacuum initial conditions (often called the Bunch-Davies vacuum).

In our case, we satisfy all the above criteria but still we generate PNGs with shapes mimicking large class of EFT models of scalar field inflation (see Sec. 6 for more details). This result of ours is completely due to non-local interactions of curvature perturbations, and therefore we reshape the so far established notions of PNGs and the primordial physics [14, 16, 28]. Below we enlist different shapes of PNGs we obtained in this model which mimic the shapes of several scalar field EFT of inflation (for each case we report here the maximum values of f_{NL} we can obtain with full detailed analysis done in Sec. 4). But contrary to the conventional models of inflation, f_{NL} in our case gets a strong scale dependence (see explanation around (4.21) to (4.26)) which allow us to distinguish our gravity theory from EFTs which we discussed in Sec. 6.

- Mimicking non-canonical single field inflation $f_{\text{NL}}^{\text{eq}} \sim f_{\text{NL}}^{\text{orth}} \sim O(10)$ and $f_{\text{NL}}^{\text{sq}} \sim O(10^{-2})$ [19]. This possibility is obtained for the case of parameter space explained in Fig. 5. PNG peaked in the equilateral template is usually recognized as a feature of a non-canonical scalar field inflation (e.g., so called DBI inflation) where the primordial curvature perturbation propagates with a non-trivial sound speed (c_s) [19]. Here we obtain this shape of PNG due to non-local interactions of curvature perturbation whose sound speed is Unity.
- Mimicking non-canonical multifield inflation with $f_{\text{NL}} \sim O(1 - 10)$ [29]. We obtain this shape of PNG in the case of non-local gravity action (3.2) with and without

²The results we report here are slightly different from [27] since our choice of formfactors is different from the one considered in [27] as explained in [1].

³By large PNGs we literally mean $f_{\text{NL}} \sim O(1 - 10)$, that is ten to hundred times higher than the prediction of standard canonical scalar field inflation [12].

the non-local cubic terms in Ricci scalar (see Fig. 2, Fig. 3 and Fig. 6). In the case without non-local cubic terms in Ricci scalar, i.e., $\lambda_c \rightarrow 0$ in (3.2), we can obtain $f_{\text{NL}} \sim O(1)$ and a robust relation between different shapes of f_{NL} stated in (5.2) which is independent of the formfactor. Furthermore, in Fig. 3 we depict a shape of PNG with $f_{\text{NL}}^{\text{eq}} \sim f_{\text{NL}}^{\text{orth}} \sim O(10)$ and $f_{\text{NL}}^{\text{sq}} \sim 1$. Notably, we violate the well-known Maldacena consistency relation for the squeezed limit $f^{\text{sq}} = \frac{5}{12}(1 - n_s)$ despite having single-field slow-roll regime. This is truly due to non-local interactions of quantum fluctuations that represents a new physics in the context of PNGs (we explained this effect in detail with a simple example in Appendix B.)

- Mimicking multifield field inflation and/or inflation with non-adiabatic initial conditions $f_{\text{NL}}^{\text{sq}} \sim f_{\text{NL}}^{\text{orth}} \sim 1$ and $f_{\text{NL}}^{\text{eq}} \sim O(10^{-2})$ [12, 17, 30]. This curious shape of PNG is obtained for the parameter space of the theory presented through Fig. 4.

All the above shapes of PNGs are obtained by changing various dimensionless parameters of the theory (3.2). We obtain various types of PNGs in a single theory with non-local purely geometric modification of gravity. This is the novel finding of this work which enforces the need to reshape our understanding of early Universe cosmology. We also computed running of various shapes of PNGs in this model in (4.26) and deduced that $\left| \frac{d \ln f_{\text{NL}}}{d \ln k} \right| \lesssim 1$ that can be one to two orders of magnitude higher than in conventional models of inflation (see Sec. 6 for details). Running PNGs could play a pivotal role in inflationary cosmology and they could be potentially detected in future CMB probes [20, 31].

All the above predictions make the generalized non-local R^2 -like inflation a viable target for future CMB and Large Scale Structure observations aimed to detect $f_{\text{NL}} \sim O(1)$ [32–36]. We argue that just the detection of $f_{\text{NL}} \sim O(1)$ does not confirm the nature of inflaton. As this work elucidates, one can generate all different PNGs within the framework of a non-local higher curvature modification of gravity. Therefore, we stress that future observations must focus on the running of PNGs in order to probe the primordial physics correctly.

3 Generalized non-local R^2 -like inflation

We briefly present here the details of generalized non-local R^2 -like inflation established in detail in [1]. The R^2 inflationary background is actually the spatially flat FLRW solution of the following eigen-value equation

$$\square R = M^2 R \tag{3.1}$$

where R is the Ricci scalar, \square is the d'Alembertian operator and M^2 is the mass of the scalaron [2]. The recent Planck observations of the scalar spectral index n_s strongly support (3.1) (that corresponds to the so-called exponential-like Plateau inflation in the Einstein frame). Motivated by this fact, in [1] a most general non-local gravity action that is com-

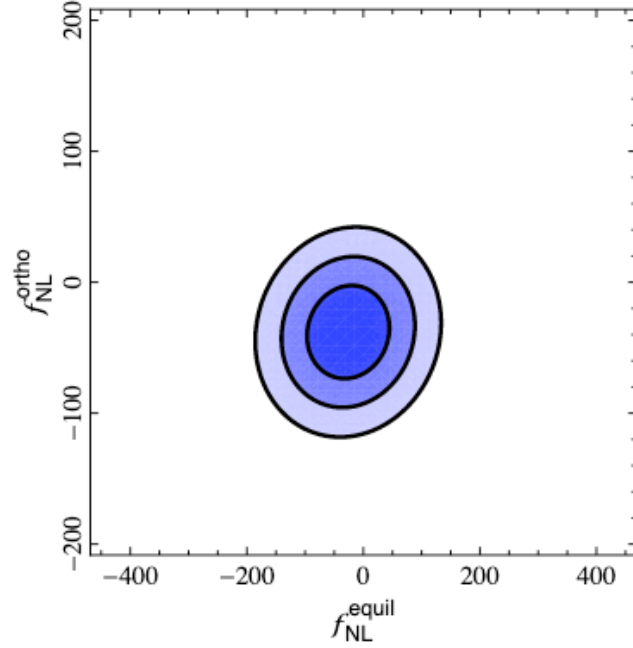


Figure 1. 68 %, 95 %, and 99.7 % confidence regions $(f_{\text{NL}}^{\text{eq}}, f_{\text{NL}}^{\text{orth}})$ taken from [14]. The predictions of generalized non-local R^2 -like inflation lie well within the bounds in this plot along with the squeezed limit PNG $-6 < f_{\text{NL}}^{\text{sq}} < 4.2$. We obtain $(f_{\text{NL}}^{\text{eq}}, f_{\text{NL}}^{\text{orth}}) \sim O(10)$, and various shapes of f_{NL} are presented in detail in Sec. 4 and Sec. 5.

patible with the R^2 inflationary background (3.1) has been constructed which is

$$\begin{aligned}
S_H^{\text{Non-local}} &= \int d^4x \sqrt{-g} L_H^{\text{Non-local}} \\
&= \int d^4x \sqrt{-g} \left(\frac{M_p^2}{2} R + \frac{1}{2} \left[R \mathcal{F}_R(\Box_s) R + \left(\frac{M_p^2}{2\mathcal{M}_s^2} + f_0 R_s \right) W_{\mu\nu\rho\sigma} \mathcal{F}_W(\Box_s, R_s) W^{\mu\nu\rho\sigma} \right. \right. \\
&\quad + \frac{f_0 \lambda_c}{\mathcal{M}_s^2} \mathcal{L}_1(\Box_s) R \mathcal{L}_2(\Box_s) R \mathcal{L}_3(\Box_s) R \\
&\quad + \frac{f_0 \lambda_R}{\mathcal{M}_s^2} \mathcal{D}_1(\Box_s) R \mathcal{D}_2(\Box_s) W^{\mu\nu\gamma\lambda} \mathcal{D}_3(\Box_s) W_{\mu\nu\gamma\lambda} \\
&\quad \left. \left. + \frac{f_0 \lambda_W}{\mathcal{M}_s^2} \mathcal{C}_1(\Box_s) W_{\mu\nu\rho\sigma} \mathcal{C}_2(\Box_s) W^{\mu\nu\gamma\lambda} \mathcal{C}_3(\Box_s) W_{\gamma\lambda}{}^{\rho\sigma} \right] + \dots \right), \tag{3.2}
\end{aligned}$$

where M_p is the reduced Planck mass, R is the Ricci scalar, $W_{\mu\nu\rho\sigma}$ is the Weyl tensor, $f_0 = \frac{M_p^2}{6M^2}$ with M being the scalaron mass, $\Box_s = \frac{\square}{\mathcal{M}_s^2}$ with \mathcal{M}_s being the so-called scale of non-locality, $R_s = \frac{R}{\mathcal{M}_s^2}$ and

$$\left\{ \mathcal{F}_R(\Box_s), \mathcal{F}_W\left(\Box_s, \frac{2R}{3\mathcal{M}_s^2}\right), \mathcal{L}_i(\Box_s), \mathcal{C}_i(\Box_s), \mathcal{D}_i(\Box_s) \right\} \tag{3.3}$$

are the formfactors which are the analytic non-polynomial functions. In [1] it was explicitly shown that these operators should take the following form in order avoid ghost degrees of freedom in the Minkowski and quasi-de Sitter (dS) limits:

$$\begin{aligned}\mathcal{F}_R(\Box_s) &= f_0 M^2 \frac{1 - \left(1 - \frac{\Box}{M^2}\right) e^{\gamma_S(\Box_s)}}{\Box_s}, \\ \mathcal{F}_W\left(\Box_s, \frac{R}{M_s^2}\right) &= \frac{e^{\gamma_T(\Box_s - \frac{2}{3}R_s)} - 1}{\Box_s - \frac{2}{3}R_s}\end{aligned}\tag{3.4}$$

where $\gamma_S(\Box_s)$ and $\gamma_T\left(\Box_s - \frac{2}{3}\frac{R}{M_s^2}\right)$ are the entire functions which can be polynomials or functions of polynomials [1]. The formfactors $\mathcal{L}_i(\Box_s)$, $\mathcal{C}(\Box_s)$, $\mathcal{D}_i(\Box_s)$ should be such that they are suppressed at the large momentum limit $p \rightarrow \infty$. These formfactors can in general contain an infinite number of arbitrary parameters, but here we assume them to be defined by a finite number of unknown parameters. Our assumption here is motivated from an expectation that any UV-complete theory can be formulated with a finite number of free parameters which can be probed by some observations. In Sec. 4 we deduce that the terms involving Weyl tensor do not contribute to the scalar PNGs which we are interested in. Therefore, the details of the operators $\mathcal{D}_i(\Box_s)$, $\mathcal{C}_i(\Box_s)$ are irrelevant to the present study. To illustrate our results of scalar PNGs, we express the operators $\mathcal{L}_i(\Box_s)$ in the following form.

$$\mathcal{L}_i(\Box_s) = e^{\ell_i(\Box_s)} - 1,\tag{3.5}$$

where $\ell_i(\Box_s)$ are the entire functions which we assume to be polynomials or functions of polynomials that gives us a finite parameter space. In order to have (3.1) as a particular exact FLRW background solution of the theory (3.2), the following conditions are sufficient [1]

$$\gamma_S\left(\frac{M^2}{\mathcal{M}_s^2}\right) = 0, \quad \ell_i\left(\frac{M^2}{\mathcal{M}_s^2}\right) = 0,\tag{3.6}$$

which we call as on-shell conditions. Since Weyl tensor is zero on FLRW backgrounds equations of motion are trivially satisfied and we do not need any conditions on $\gamma_T\left(\Box_s - \frac{2}{3}\frac{R}{M_s^2}\right)$, $\mathcal{C}_i(\Box_s)$ and $\mathcal{D}_i(\Box_s)$ at the background level. From (3.6) we can write a generic form of entire functions as

$$\begin{aligned}\gamma_S(\Box_s) &= \left(\Box_s - \frac{M^2}{\mathcal{M}_s^2}\right) P_S(\Box_s), \\ \ell_i(\Box_s) &= \left(\Box_s - \frac{M^2}{\mathcal{M}_s^2}\right) G_i(\Box_s)\end{aligned}\tag{3.7}$$

where $P_S(\Box_s)$, $G_i(\Box_s)$ are the finite degree polynomials such that the operators $\mathcal{L}_i\left(\frac{p^2}{\mathcal{M}_s^2}\right)$ do not grow in the limit $p \rightarrow \infty$, for the theory to be consistent in the UV-regime and to apply it safely to the low-energy context which is inflation in our case. As a result, the parameter space of the theory (3.2) is finite dimensional although the action (3.2) is non-local (i.e., infinite derivative) in nature. It was shown in [1] that the cubic non-local scalar curvature term does not contribute to the second order perturbed action but this term does contribute to the third order perturbed action that will be explained in the next

section. Furthermore, we would like to emphasize here the PNGs we compute and report in the later sections are fully compatible with the predictions of scalar and tensor power spectrum and their tilts reported in [1]. Finally, note that the terms denoted by \dots in (3.2) are the higher order non-local scalar curvature and Weyl curvature terms which we assume to be not relevant for the 3-point inflationary correlations (see the discussion around (4.9)).

4 PNGs and their running in generalized non-local R^2 -like inflation

This section is dedicated to computing scalar PNGs of R^2 -like inflation in our higher curvature non-local action (3.2). We make use of several calculations in this regard from the previous study [27] where the computation of PNGs in non-local theories was robustly developed. Let us start with recalling some standard procedure and definitions related to the computation of 3-point correlations which are defined by [27, 37]

$$\langle \mathcal{R}(\mathbf{k}_1) \mathcal{R}(\mathbf{k}_2) \mathcal{R}(\mathbf{k}_3) \rangle = -i \int_{-\infty}^{\tau_e} d\tau \langle 0 | [\mathcal{R}(\tau_e, \mathbf{k}_1) \mathcal{R}(\tau_e, \mathbf{k}_2) \mathcal{R}(\tau_e, \mathbf{k}_3), H_{int}] | 0 \rangle, \quad (4.1)$$

where \mathbf{k}_i are wave vectors and $H_{int} \approx -\mathcal{L}_3$ is the interaction Hamiltonian that is approximately equal to the 3rd order perturbation of the Lagrangian (3.2) (\mathcal{L}_3) within the slow-roll approximation [37, 38] and τ_e denotes the end of inflation.

The so-called bi-spectrum ($\mathcal{B}_{\mathcal{R}}$) is defined as

$$\langle \mathcal{R}(\mathbf{k}_1) \mathcal{R}(\mathbf{k}_2) \mathcal{R}(\mathbf{k}_3) \rangle = (2\pi)^3 \delta^3(\mathbf{k}_1 + \mathbf{k}_2 + \mathbf{k}_3) \mathcal{B}_{\mathcal{R}}(k_1, k_2, k_3) \quad (4.2)$$

where $|\mathbf{k}_i| = k_i$ and the non-linear curvature perturbation \mathcal{R} is expressed as [39, 40]

$$\mathcal{R} = \mathcal{R}_g - \frac{3}{5} f_{NL} (\mathcal{R}_g^2 - \langle \mathcal{R}_g \rangle^2), \quad (4.3)$$

where \mathcal{R}_g being the Gaussian random field and the f_{NL} is the non-linearity parameter also known as the reduced bi-spectrum [13]. f_{NL} is related to the amplitude of the bi-spectrum $A_{\mathcal{R}}(k_1, k_2, k_3)$ as

$$f_{NL} = -\frac{5}{6} \frac{A_{\mathcal{R}}(k_1, k_2, k_3)}{\sum_i k_i^3}, \quad (4.4)$$

where $A_{\mathcal{R}}(k_1, k_2, k_3)$ stands for the redefinition of the bi-spectrum $B_{\mathcal{R}}$:

$$B_{\mathcal{R}}(k_1, k_2, k_3) = 4\pi^4 \frac{1}{\prod_i k_i^3} \mathcal{P}_{\mathcal{R}}^2 A_{\mathcal{R}}(k_1, k_2, k_3). \quad (4.5)$$

Here $\mathcal{P}_{\mathcal{R}}$ is the power spectrum of curvature perturbation [1]

$$\mathcal{P}_{\mathcal{R}} \approx \frac{1}{3f_0 \bar{R}_{\text{dS}}} \frac{H^2}{16\pi^2 \epsilon^2} \quad (4.6)$$

where H is the Hubble parameter during inflation and $\epsilon = -\frac{\dot{H}}{H^2} \approx \frac{1}{2N}$ with $N \gg 1$ where N represents the number of e-folds. To calculate f_{NL} , we consider the third order variation of (3.2) around the background (3.1) which can be computed as

$$\delta_{(s)}^{(3)} S_H^{\text{Non-local}} = \delta_{(s)}^{(3)} S_{R+R^2}^{\text{local}} + \delta_{(s)}^{(3)} S_{R+R^2}^{\text{Non-local}} + \delta_{(s)}^{(3)} S_{\mathbb{R}^3}^{\text{Non-local}} \quad (4.7)$$

where

$$\begin{aligned}
S_{R+R^2}^{\text{local}} &= \int d^4x \sqrt{-g} \left[\frac{M_p^2}{2} R + \frac{f_0}{2} R^2 \right] \\
S_{R+R^2}^{\text{Non-local}} &= \int d^4x \sqrt{-g} \left\{ \frac{M_p^2}{2} R + \frac{1}{2} R \left[\mathcal{F}_R(\square_s) - f_0 \right] R \right\} \\
S_{R^3}^{\text{Non-local}} &= \int d^4x \sqrt{-g} \left[\mathcal{L}_1(\square_s) R \mathcal{L}_2(\square_s) R \mathcal{L}_3(\square_s) R \right]
\end{aligned} \tag{4.8}$$

and the subscript (s) in (4.7) denotes that we only consider 3-point scalar correlations, so we are dropping all interactions containing tensor modes. Using the calculations performed in [27], since $\Phi + \Psi \approx 0$ during inflation and the variation $\delta_{(s)} W_{\mu\nu\rho\sigma} \propto \Phi + \Psi$, we can conclude that all the terms involving Weyl tensor do not contribute to the scalar PNGs. In (3.2), we can further consider quartic order non-local scalar curvature term:

$$S_{R^4}^{\text{Non-local}} = \frac{f_0 \lambda_q}{2 \mathcal{M}_s^4} \int d^4x \sqrt{-g} \left[\mathcal{L}_4(\square_s) R \mathcal{L}_1(\square_s) R \mathcal{L}_2(\square_s) R \mathcal{L}_2(\square_s) R \right]. \tag{4.9}$$

Here $\mathcal{L}_4(\square_s)$ is an arbitrary analytic infinite derivative operator. It is easy to deduce that (4.9) still admits the inflationary solution (3.1). Applying $\mathcal{L}_i \left(\frac{M^2}{\mathcal{M}_s^2} \right) = 0$ ($i = 1, 2, 3$), we can conclude that the second order variation of (4.9) around the background satisfying (3.1) becomes zero exactly

$$\delta^{(2)} S_{R^4}^{\text{Non-local}} = 0, \tag{4.10}$$

whereas the 3rd order variation of (4.9) around (3.1) in the leading order de Sitter approximation is

$$\delta^{(3)} S_{R^4}^{\text{Non-local}} \approx \mathcal{L}_4 \left(\frac{M^2}{\mathcal{M}_s^2} \right) \frac{\lambda_q \bar{R}_{\text{dS}}}{\lambda_c \mathcal{M}_s^2} \delta^{(3)} S_{R^3}^{\text{Non-local}}. \tag{4.11}$$

Given we assume

$$\mathcal{L}_4 \left(\frac{M^2}{\mathcal{M}_s^2} \right) \frac{\lambda_q \bar{R}_{\text{dS}}}{\lambda_c \mathcal{M}_s^2} \ll 1, \tag{4.12}$$

we can neglect the contribution of (4.9) to scalar (3-point) PNGs. However, we can possibly have non-negligible contributions to the trispectrum (or) 4-point correlations due to this term. The same logic can be easily extended to other higher scalar curvature non-local terms. Similarly, we can add quartic in Weyl tensor terms to (3.2) which do not contribute to the 3-point inflationary correlations due to the fact that background Weyl tensor vanishes in FLRW.

Therefore, non-local contributions to the bispectrum arise only from the part of the action (3.2) which is quadratic and cubic in Ricci scalar. PNGs from the non-local quadratic term in Ricci scalar were computed in [27]. We borrow and present here these results with two important changes. First, we include the contributions that explicitly break the scale invariance of the bispectrum. These contributions are important for studying the running of PNGs that we compute in the next section. Second, we present PNGs for the formfactors we introduced in (3.4). In Appendix A we compute PNGs arising from the non-local cubic in Ricci scalar term which gives new shapes of PNGs that we shall discuss in the next

section. Finally, we obtain the 3rd order action (4.7) in terms of the curvature perturbation \mathcal{R} in the leading order slow-roll approximation as

$$\delta_{(s)}^{(3)} S_H^{\text{Non-local}} = 4\epsilon M_p^2 \int d\tau d^3x \left\{ B_1 \mathcal{R} \nabla \mathcal{R} \cdot \nabla \mathcal{R} + B_2 \mathcal{R} \mathcal{R}'^2 + B_3 \mathcal{H} \mathcal{R} \mathcal{R} \mathcal{R}' \right. \\ \left. + B_4 \mathcal{H}^{-1} \mathcal{R}'^3 + B_5 \mathcal{H}^2 \mathcal{R}^3 B_6 \mathcal{H}^{-1} \nabla \mathcal{R} \cdot \nabla \mathcal{R} \mathcal{R}' + B_7 \mathcal{H}^{-2} \mathcal{R}' \nabla \mathcal{R} \cdot \nabla \mathcal{R}' \right\}, \quad (4.13)$$

where B_1 to B_7 are dimensionless parameters approximated to be constant during inflation which are given by

$$\begin{aligned} B_1 &= -2\epsilon - \frac{3\epsilon^2}{4} \\ B_2 &= 2\epsilon + \frac{3\epsilon^2}{4} + \frac{16\bar{R}_{\text{dS}}}{3M_p^2} \epsilon \mathcal{T}_{\text{NL}} + \frac{4\bar{R}_{\text{dS}}^2}{M_p^2 \mathcal{M}_s^2} - \frac{2\lambda_c}{9} \frac{\bar{R}_{\text{dS}}}{\mathcal{M}_s^2} \epsilon (2\epsilon^2 T_{\text{NL}}^3 + \epsilon T_{\text{NL}}^2 + T_{\text{NL}}^1) \\ B_3 &= -\frac{32\bar{R}_{\text{dS}}}{M_p^2} \epsilon^3 \mathcal{T}_{\text{NL}} - \frac{8\lambda_c}{9} \frac{\bar{R}_{\text{dS}}}{\mathcal{M}_s^2} \epsilon (2\epsilon T_{\text{NL}}^2 + T_{\text{NL}}^1) \\ B_4 &= -\frac{2\bar{R}_{\text{dS}}}{M_p^2} \epsilon^3 \mathcal{T}_{\text{NL}} - \frac{1}{54} \frac{\bar{R}_{\text{dS}}}{\mathcal{M}_s^2} \epsilon (8\epsilon^3 T_{\text{NL}}^4 + 4\epsilon^2 T_{\text{NL}}^3 + 2\epsilon T_{\text{NL}}^2 + T_{\text{NL}}^1) \\ B_5 &= -\frac{\epsilon^2}{2} + \frac{32\bar{R}_{\text{dS}}}{\mathcal{M}_s^2} \epsilon T_{\text{NL}}^1 \\ B_6 &= \frac{2\bar{R}_{\text{dS}}}{M_p^2} \mathcal{T}_{\text{NL}} \\ B_7 &= \frac{16\bar{R}_{\text{dS}}}{3M_p^2} \epsilon^4 \mathcal{T}_{\text{NL}} + \frac{4\bar{R}_{\text{dS}}^2}{3M_p^2 \mathcal{M}_s^2} \epsilon^4 \mathcal{F}_R^{(\dagger)} \left(\frac{\bar{R}_{\text{dS}}}{4\mathcal{M}_s^2} \right), \end{aligned} \quad (4.14)$$

where the subscript “dS” denotes the quantities in quasi-dS approximation.

$$\mathcal{T}_{\text{NL}} = \epsilon^2 \left(e^{\gamma_S \left(\frac{\bar{R}_{\text{dS}}}{\mathcal{M}_s^2} \right)} - 1 \right) + \epsilon^3 \frac{\bar{R}_{\text{dS}}^2}{4\mathcal{M}_S^4} \gamma_S^\dagger \left(\frac{\bar{R}_{\text{dS}}}{\mathcal{M}_s^2} \right) e^{\gamma_S \left(\frac{\bar{R}_{\text{dS}}}{\mathcal{M}_s^2} \right)} \quad (4.15)$$

is obtained from the definition (A.7) for the formfactor $\mathcal{F}_R(\square_s)$ in (3.4). And the quantities $T_{\text{NL}}^1, \dots, T_{\text{NL}}^4$ are defined in (A.8).

Computing the amplitude of 3-point correlation, we obtain

$$A_{\mathcal{R}} = \sum_{i=1}^7 B_i S_i, \quad (4.16)$$

where

$$\begin{aligned} S_1 &= 2\mathbf{k}_1 \cdot \mathbf{k}_2 \left[K - \frac{k_1 k_2 + k_2 k_3 + k_3 k_1}{K} - \frac{k_1 k_2 k_3}{K^2} \right] + \text{perms}, \\ S_2 &= \frac{2k_1^2 k_2^2}{K} + \frac{2k_1^2 k_2^2 k_3}{K^2} + \text{perms}, \\ S_3 &\approx k_3^2 \left[-2K - \frac{2k_1 k_2}{K} \right] + \mathcal{C}(z) k_3^3 + \text{perms} \end{aligned} \quad (4.17)$$

$$\begin{aligned}
S_4 &= \frac{4k_1^2 k_2^2 k_3^2}{K^3} + \text{perms} \\
S_5 &= -\frac{K^3}{3} + 2Kk_1k_2 + \frac{k_1k_2k_3}{3} + \text{perms} \\
S_6 &= 2(\mathbf{k}_1 \cdot \mathbf{k}_2) k_3^2 \left[\frac{2}{K} + \frac{2k_1 + 2k_2}{K^2} + \frac{4k_1k_2}{K^3} \right] + \text{perms} \\
S_7 &= (\mathbf{k}_2 \cdot \mathbf{k}_3) k_1^2 k_3^2 \left[-\frac{2}{K^3} - \frac{6k_2}{K^4} \right]
\end{aligned} \tag{4.18}$$

where $z = \frac{K}{K_*}$ with $K_* = a_* H_* = 0.05 \text{ Mpc}^{-1}$ is a particular reference scale and $C(z) \approx \gamma_E + \ln z - \frac{z^2}{4} + \frac{z^4}{96}$. In deriving (4.13), we used the following on shell relations which are the result of the background solution (3.1) and the equation of motion for curvature perturbation at the linearized level [27, 41]:

$$\begin{aligned}
\bar{\square}_s \mathcal{R} &\approx \frac{M^2}{\mathcal{M}_s^2} \mathcal{R} \implies \mathcal{O}(\bar{\square}_s) \mathcal{R} \approx \mathcal{O}\left(\frac{M^2}{\mathcal{M}_s^2}\right) \mathcal{R} \\
\bar{\square}_s \mathcal{R}' &\approx \left(\frac{\bar{\square}_s}{\mathcal{M}_s^2} + \frac{\bar{R}_{\text{dS}}}{4\mathcal{M}_s^2} \right) \mathcal{R}' \implies \mathcal{O}(\bar{\square}_s) \mathcal{R}' \approx \mathcal{O}\left(\frac{M^2}{\mathcal{M}_s^2} + \frac{\bar{R}_{\text{dS}}}{4\mathcal{M}_s^2}\right) \mathcal{R}',
\end{aligned} \tag{4.19}$$

where \mathcal{O} is an arbitrary analytic operator. The above on-shell relations together with (3.1) bring the 3rd order action of the non-local gravity (3.2) into the local form, and all the effect of non-localities is transferred into the on-shell vertex factors \mathcal{T}_{NL} and $T_{\text{NL}}^1, \dots, T_{\text{NL}}^4$.

4.1 Shape of $f_{\text{NL}}(k_1, k_2, k_3)$ and its running n_{NG}

In this section, we explore various shapes of the reduced bispectrum $f_{\text{NL}}(k_1, k_2, k_3)$ and their running [13, 19, 42] which are very significant observables to probe the nature of the scalar field (either scalaron or inflaton) and its interactions⁴. Discussion of results obtained in this section are presented in Sec. 2 and Sec. 6. The shape of PNGs can quantified by plotting $f_{\text{NL}}(k_1, k_2, k_3)$ in terms of the following redefinition of wave-numbers [42, 43]:

$$k_1 = \frac{1}{4}(\alpha_s + \beta_s + K), \quad k_2 = \frac{1}{4}(-\alpha_s + \beta_s + K), \quad k_3 = \frac{1}{2}(K - \beta_s). \tag{4.20}$$

If future observations will probe fully the functional dependence of $f_{\text{NL}}(K, \alpha_s, \beta_s)$, we can fully determine self-interactions of the scalarons we see in (4.7) which are by nature not scale-invariant. PNGs of the generalized non-local R^2 -like inflation (3.2) are computed by substituting (4.16) in (4.4). There are three shapes of reduced bi-spectrum called “equilateral: $k_1 = k_2 = k_3 = k/3$ ”, “orthogonal: $4k_1 = 4k_2 = 2k_3 = k$ ”, “squeezed: $k_3 \ll k_1 = k_2 = \frac{k}{2}$ ” (where the total momentum $K = k$) which are more relevant popular templates with the

⁴There are several ways one can define the shape of bispectrum [12]. One definition of the shape function is $S(k_1, k_2, k_3) = \frac{f_{\text{NL}}(k_1, k_2, k_3)}{k_1 k_2 k_3}$ [12]. In this paper, we stick to the shape function defined by the reduced bispectrum $f_{\text{NL}}(k_1, k_2, k_3)$ [13].

present CMB constraints [18]. Computing f_{NL} for these three configurations, we obtain

$$\begin{aligned}
f_{\text{NL}}^{\text{sq}} &\approx \frac{5}{12} (1 - n_s) - 35.5 \mathcal{T}_{\text{NL}} + 8.9 \mathcal{C}(z) \mathcal{T}_{\text{NL}} - 1.1 \epsilon^3 \frac{\bar{R}_{\text{dS}}^2}{\mathcal{M}_s^4} \gamma_S^\dagger \left(\frac{\bar{R}_{\text{dS}}}{\mathcal{M}_s^2} \right) \\
&\quad - \lambda_c \frac{\bar{R}_{\text{dS}}}{\mathcal{M}_s^2} \left(5.8 \epsilon^2 T_{\text{NL}}^2 - 1.5 \mathcal{C}(z) \epsilon^2 T_{\text{NL}}^2 - 0.19 \epsilon^3 T_{\text{NL}}^3 \right), \\
f_{\text{NL}}^{\text{equiv}} &\approx \frac{5}{12} (1 - n_s) - 46.6 \mathcal{T}_{\text{NL}} + 8.9 \mathcal{C}(z) \mathcal{T}_{\text{NL}} - 1.8 \epsilon^3 \frac{\bar{R}_{\text{dS}}^2}{\mathcal{M}_s^4} \gamma_S^\dagger \left(\frac{\bar{R}_{\text{dS}}}{\mathcal{M}_s^2} \right) \\
&\quad - \lambda_c \frac{\bar{R}_{\text{dS}}}{\mathcal{M}_s^2} \left(7.7 \epsilon^2 T_{\text{NL}}^2 - 1.5 \mathcal{C}(z) \epsilon^2 T_{\text{NL}}^2 - 0.3 \epsilon^3 T_{\text{NL}}^3 - 0.02 \epsilon^4 T_{\text{NL}}^4 \right), \\
f_{\text{NL}}^{\text{ortho}} &\approx \frac{5}{12} (1 - n_s) - 39.1 \mathcal{T}_{\text{NL}} + 8.9 \mathcal{C}(z) \mathcal{T}_{\text{NL}} - 1.2 \epsilon^3 \frac{\bar{R}_{\text{dS}}^2}{\mathcal{M}_s^4} \gamma_S^\dagger \left(\frac{\bar{R}_{\text{dS}}}{\mathcal{M}_s^2} \right) \\
&\quad - \lambda_c \frac{\bar{R}_{\text{dS}}}{\mathcal{M}_s^2} \left(6.4 \epsilon^2 T_{\text{NL}}^2 - 1.5 \mathcal{C}(z) \epsilon^2 T_{\text{NL}}^2 - 0.2 \epsilon^3 T_{\text{NL}}^3 - 0.01 \epsilon^4 T_{\text{NL}}^4 \right).
\end{aligned} \tag{4.21}$$

From (4.21) we can conclude that all the crucial f_{NL} configurations get non-local contributions. There are three types of non-local contributions appearing in the expressions (4.21).

1. Contributions involving $e^{\gamma_S(\square_s)}$ come from the term that is quadratic in scalar curvature (4.8) for the formfactor $\mathcal{F}_R(\square_s)$ (3.4).
2. Contribution from the cubic non-local scalar curvature term (4.8): this can be read from the terms involving $T_{\text{NL}}^2 - T_{\text{NL}}^4$. As explained in Appendix A, we found the contributions of the terms involving T_{NL}^1 are negligible compared to other terms and therefore we drop them in (4.21) for brevity.
3. Contribution involving $\mathcal{C}\left(\frac{K}{K_*}\right)$ which comes from taking carefully the infrared (IR) limit of integration using the judicious choice $\tau = -\frac{1}{K_*}$ [44, 45]. Usually this contribution is slow-roll suppressed in standard single field models of inflation [19, 45, 46], but in our case it is modulated by analytic non-local contributions⁵ when $\bar{R} \gtrsim \mathcal{M}_s^2$.

From (4.21) we can deduce that the non-Gaussianity parameter f_{NL} that can be potentially observable in future depends on the following set of quantities

$$\left\{ e^{\gamma_S\left(\frac{\bar{R}_{\text{dS}}}{4\mathcal{M}_s^2}\right)}, \gamma_S^\dagger\left(\frac{\bar{R}_{\text{dS}}}{4\mathcal{M}_s^2}\right), \lambda_c, e^{\ell_i\left(\frac{\bar{R}_{\text{dS}}}{4\mathcal{M}_s^2}\right)} \right\}. \tag{4.22}$$

As we discussed in the previous section, the scale invariance of bispectrum (4.16) is broken in the non-local R^2 -like inflation due to the scale dependence of quantities (4.22) through

$$\left\{ \bar{R}_{\text{dS}}(k), \mathcal{C}(k) \right\} \tag{4.23}$$

⁵In our result (4.21) we neglected small local contributions of the order $O(\epsilon^2)$.

Due to the presence of exponentials, we can expect that the scale dependence can be significant. To quantify it we define a new parameter called running of f_{NL} as [19]

$$n_{\text{NG}} \equiv \frac{d \ln f_{\text{NL}}}{d \ln k} \quad (4.24)$$

which we can evaluate in the various limits such as squeezed, equilateral and orthogonal. The n_{NG} can be evaluated using the following quantities

$$\begin{aligned} \frac{df_{\text{NL}}^{\text{sq}}}{d \ln k} \approx & -\frac{dn_s}{d \ln k} + \left(-35.5 + 8.9 \mathcal{C}(z) \right) \frac{\partial \mathcal{T}_{\text{NL}}}{\partial N} + \mathcal{C}^\dagger(z) \left(8.9 \mathcal{T}_{\text{NL}} + \epsilon^2 \lambda_c \frac{\bar{R}_{\text{dS}}}{\mathcal{M}_s^2} T_{\text{NL}}^2 \right) \\ & - 2.2 \epsilon^4 \frac{\bar{R}_{\text{dS}}^3}{\mathcal{M}_s^3} \left[\gamma_S^\dagger \left(\frac{\bar{R}_{\text{dS}}}{\mathcal{M}_s^2} \right) + \frac{1}{4} \gamma_S^{\dagger 2} \left(\frac{\bar{R}_{\text{dS}}}{\mathcal{M}_s^2} \right) + \frac{1}{4} \gamma_S^{\dagger \dagger} \left(\frac{\bar{R}_{\text{dS}}}{\mathcal{M}_s^2} \right) \right] \\ & - \epsilon \lambda_c \frac{2 \bar{R}_{\text{dS}}}{\mathcal{M}_s^2} \left(5.8 \epsilon^2 T_{\text{NL}}^2 - 1.5 \epsilon^2 \mathcal{C}(z) T_{\text{NL}}^2 - 0.76 \epsilon^3 T_{\text{NL}}^3 \right) \\ & + \epsilon \lambda_c \frac{\bar{R}_{\text{dS}}^2}{2 \mathcal{M}_s^4} \left(5.8 \epsilon^2 \frac{\partial T_{\text{NL}}^2}{\partial N} - 1.5 \epsilon^2 \mathcal{C}(z) \frac{\partial T_{\text{NL}}^2}{\partial N} - 0.19 \epsilon^3 \frac{\partial T_{\text{NL}}^3}{\partial N} \right), \end{aligned} \quad (4.25)$$

$$\begin{aligned} \frac{df_{\text{NL}}^{\text{eq}}}{d \ln k} \approx & -\frac{dn_s}{d \ln k} + \left(-46.6 + 8.9 \mathcal{C}(z) \right) \frac{\partial \mathcal{T}_{\text{NL}}}{\partial N} + \mathcal{C}^\dagger(z) \left(8.9 \mathcal{T}_{\text{NL}} + \epsilon^2 \lambda_c \frac{\bar{R}_{\text{dS}}}{\mathcal{M}_s^2} T_{\text{NL}}^2 \right) \\ & - 3.6 \epsilon^4 \frac{\bar{R}_{\text{dS}}^3}{\mathcal{M}_s^3} \left[\gamma_S^\dagger \left(\frac{\bar{R}_{\text{dS}}}{\mathcal{M}_s^2} \right) + \frac{1}{4} \gamma_S^{\dagger 2} \left(\frac{\bar{R}_{\text{dS}}}{\mathcal{M}_s^2} \right) + \frac{1}{4} \gamma_S^{\dagger \dagger} \left(\frac{\bar{R}_{\text{dS}}}{\mathcal{M}_s^2} \right) \right] \\ & - \epsilon \lambda_c \frac{2 \bar{R}_{\text{dS}}}{\mathcal{M}_s^2} \left(7.7 \epsilon^2 T_{\text{NL}}^2 - 1.5 \epsilon^2 \mathcal{C}(z) T_{\text{NL}}^2 - 1.2 \epsilon^3 T_{\text{NL}}^3 - 0.12 \epsilon^4 T_{\text{NL}}^4 \right) \\ & + \epsilon \lambda_c \frac{\bar{R}_{\text{dS}}^2}{2 \mathcal{M}_s^4} \left(7.7 \epsilon^2 \frac{\partial T_{\text{NL}}^2}{\partial N} - 1.5 \epsilon^2 \mathcal{C}(z) \frac{\partial T_{\text{NL}}^2}{\partial N} - 0.3 \epsilon^3 \frac{\partial T_{\text{NL}}^3}{\partial N} - 0.02 \epsilon^4 \frac{\partial T_{\text{NL}}^4}{\partial N} \right), \end{aligned}$$

$$\begin{aligned} \frac{df_{\text{NL}}^{\text{orth}}}{d \ln k} \approx & -\frac{dn_s}{d \ln k} + \left(-39.1 + 8.9 \mathcal{C}(z) \right) \frac{\partial \mathcal{T}_{\text{NL}}}{\partial N} + \mathcal{C}^\dagger(z) \left(8.9 \mathcal{T}_{\text{NL}} + \epsilon^2 \lambda_c \frac{\bar{R}_{\text{dS}}}{\mathcal{M}_s^2} T_{\text{NL}}^2 \right) \\ & - 2.4 \epsilon^4 \frac{\bar{R}_{\text{dS}}^3}{\mathcal{M}_s^3} \left[\gamma_S^\dagger \left(\frac{\bar{R}_{\text{dS}}}{\mathcal{M}_s^2} \right) + \frac{1}{4} \gamma_S^{\dagger 2} \left(\frac{\bar{R}_{\text{dS}}}{\mathcal{M}_s^2} \right) + \frac{1}{4} \gamma_S^{\dagger \dagger} \left(\frac{\bar{R}_{\text{dS}}}{\mathcal{M}_s^2} \right) \right] \\ & - \epsilon \lambda_c \frac{2 \bar{R}_{\text{dS}}}{\mathcal{M}_s^2} \left(6.4 \epsilon^2 T_{\text{NL}}^2 - 1.5 \epsilon^2 \mathcal{C}(z) T_{\text{NL}}^2 - 0.8 \epsilon^3 T_{\text{NL}}^3 - 0.06 \epsilon^4 T_{\text{NL}}^4 \right) \\ & + \epsilon \lambda_c \frac{\bar{R}_{\text{dS}}^2}{2 \mathcal{M}_s^4} \left(6.4 \epsilon^2 \frac{\partial T_{\text{NL}}^2}{\partial N} - 1.5 \mathcal{C}(z) \epsilon^2 \frac{\partial T_{\text{NL}}^2}{\partial N} - 0.2 \epsilon^3 \frac{\partial T_{\text{NL}}^3}{\partial N} - 0.01 \epsilon^4 \frac{\partial T_{\text{NL}}^4}{\partial N} \right). \end{aligned} \quad (4.26)$$

From (4.26) we can deduce that running of PNGs depend on the higher derivatives of our formfactors (4.22). This reveals that if we measure running of PNGs in future observations, we can probe the formfactors, reconstruct our theory and ultimately learn about UV-completion of gravity.

4.2 Quantum fluctuations and the bi-spectrum

In [1] it was shown that the sound speed of curvature perturbations is Unity in the non-local gravity inflation (3.2). Therefore, we have an effective scalar field (scalaron) propagating during inflation similar to the local R^2 theory. Moreover, it was shown in [1] that there is only a single scalar mode that is propagating during inflation. Thus, we can also conclude that the leading mode of the curvature perturbations \mathcal{R} , corresponding to the growing mode of energy density perturbations, is approximately time-independent on super-Hubble scales while the generic solution for \mathcal{R} there has the form [47]

$$\mathcal{R} = c_1 + c_2 \int \frac{dt}{a^3 \epsilon}. \quad (4.27)$$

This implies all the PNGs which are generated in the generalized non-local R^2 -like inflation are determined by interactions of quantum fluctuations which evolve until the moment of the Hubble radius crossing during inflation that is exactly what we compute here. Obviously since all the modes become frozen on super-Hubble scales $k \ll aH$, the f_{NL} are solely determined by quantum field interactions when $k \sim aH$. We will see in the next subsection that non-local self interactions of \mathcal{R} can generate sizeable contributions for all f_{NL} in squeezed, equilateral and orthogonal configurations when the non-locality scale is close to the Hubble scale during inflation $\mathcal{M}_s \gtrsim H$. As we noted before, non-commutativity of covariant and partial derivatives in the quasi-dS regime (4.19) plays a crucial role in getting large PNGs in the generalized non-local R^2 -like inflation. This result evades all known ways of obtaining detectable level of PNGs through non-canonical scalar field(s) and not adiabatic vacuum (or, non-Bunch-Davis) initial conditions [12]. Most notably, we modify the Maldacena consistency relation that was argued to take place for any general single field standard slow-roll inflation [10, 46, 48]. We further discuss this in detail later in Sec. 6 and Appendix B.

5 Numerical illustration for shapes of f_{NL} and their running $n_{f_{\text{NL}}}$

To illustrate our result with explicit numbers, we plot f_{NL} values for different shapes choosing the following entire functions $\ell_i(\Box_s)$ that are compatible with (3.6)

$$\gamma_S(\Box_s) = \alpha_1 \Box_s \left(\Box_s - \frac{M^2}{\mathcal{M}_s^2} \right) + \dots, \quad \ell_i(\Box_s) = \alpha_{i1} \Box_s \left(\Box_s - \frac{M^2}{\mathcal{M}_s^2} \right) + \dots, \quad (5.1)$$

where α_1, α_{i1} are 4 dimensionless parameters. The \dots represent higher order terms which we assume to be irrelevant at the inflationary scales, but they are important to suppress formfactors in the infinite momentum limit $p \rightarrow \pm\infty$. The results we report here are not that much sensitive to the choice (5.1), and in principle we can consider higher degree polynomials in \Box_s for $\gamma_S(\Box_s), \ell_i(\Box_s)$, but choosing (5.1) we explicitly assume the effect of higher order terms in \Box_s to be negligible by setting the dimensionless coefficients of them $\ll (\alpha_1, \alpha_{i1})$. We assume $\alpha_{i1} \sim O(1-10)$, so that we do not fine tune much our free parameters and we can rely on the scale of non-locality \mathcal{M}_s for physics discussion.

5.1 The case with only non-local quadratic term in curvature scalar: $\lambda_c = 0$

In this section, we analyse the PNGs of a case without the cubic non-local Ricci scalar term in (3.2) by setting $\lambda_c = 0$. Our results for the various shapes of f_{NL} in this case lead to universal relations between them that do not explicitly depend on any choice of $\gamma_S (\Box_s)$:

$$f_{\text{NL}}^{\text{eq}} \approx 1.5 f_{\text{NL}}^{\text{sq}}, \quad f_{\text{NL}}^{\text{orth}} \approx 1.1 f_{\text{NL}}^{\text{sq}}. \quad (5.2)$$

They can be verified through the expressions in (4.21) evaluating them at $k = k_*$, and when the non-local contribution dominates over $\frac{5}{12}(1 - n_s)$. We can also verify this numerically in Fig. 2 where we also plot the running of f_{NL} defined in (4.24). It is seen from it that (5.2) is satisfied while running of f_{NL} does not follow this relation because running depends on the quantity $\mathcal{C}^\dagger(z)$ explicitly.

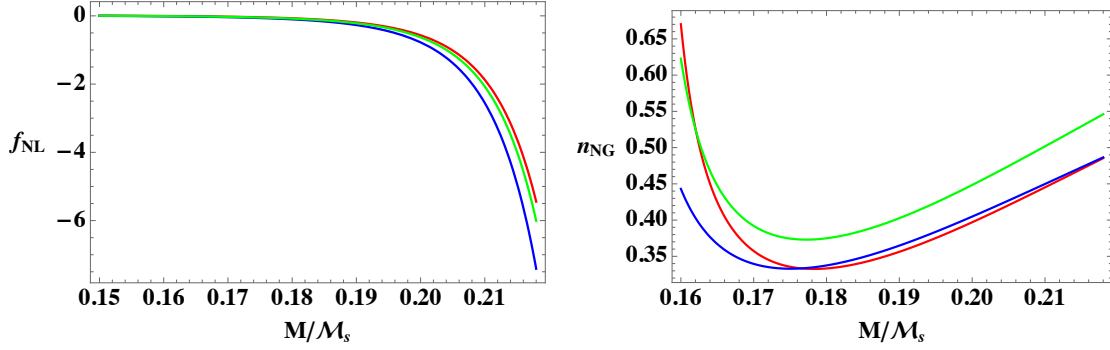


Figure 2. In the left panel we plot $f_{\text{NL}}^{\text{sq}}, f_{\text{NL}}^{\text{eq}}, f_{\text{NL}}^{\text{orth}}$ versus M/M_s (in red, blue and green coloured lines respectively) and in the right panel we plot the corresponding running of f_{NL} . In both of the plots, we take $\alpha_1 = 1$, $\lambda_c = 0$ and $N = 55$ corresponding to the pivot scale $k_* = a_* H_*$. In these plots we recover the predictions of local R^2 gravity in the limit $\frac{M}{\mathcal{M}_s} \rightarrow 0$.

5.2 New shapes and running of PNGs with all the terms in (3.2)

In this section, we illustrate numerically the various shapes of PNGs that arise in the generalized non-local R^2 -like inflation. With $\lambda_c \neq 0$ we obtain new shapes of PNGs mimicking several classes of scalar field models of inflation and EFTs discussed in Sec. 2 and Sec. 6. All of these distinct shapes are obtained for various values of parameters (α_1, α_{i1}) .

1. Large PNGs compatible with the Planck constraints (1.1): see Fig. 3.
2. Large PNGs in the squeezed and orthogonal limit while negligible in the equilateral limit: see Fig. 4.
3. Large PNGs in the equilateral and orthogonal limit while negligible in the squeezed limit: see Fig. 5.
4. Large PNGs with equal contributions in the squeezed equilateral, orthogonal limits: see Fig. 6.

Finally we plot the full shape of $f_{\text{NL}}(1, \alpha_s, \beta_s)$ in (7) as a function of (α_s, β_s) defined in (4.20) considering the same parameter values used in Fig. 3.

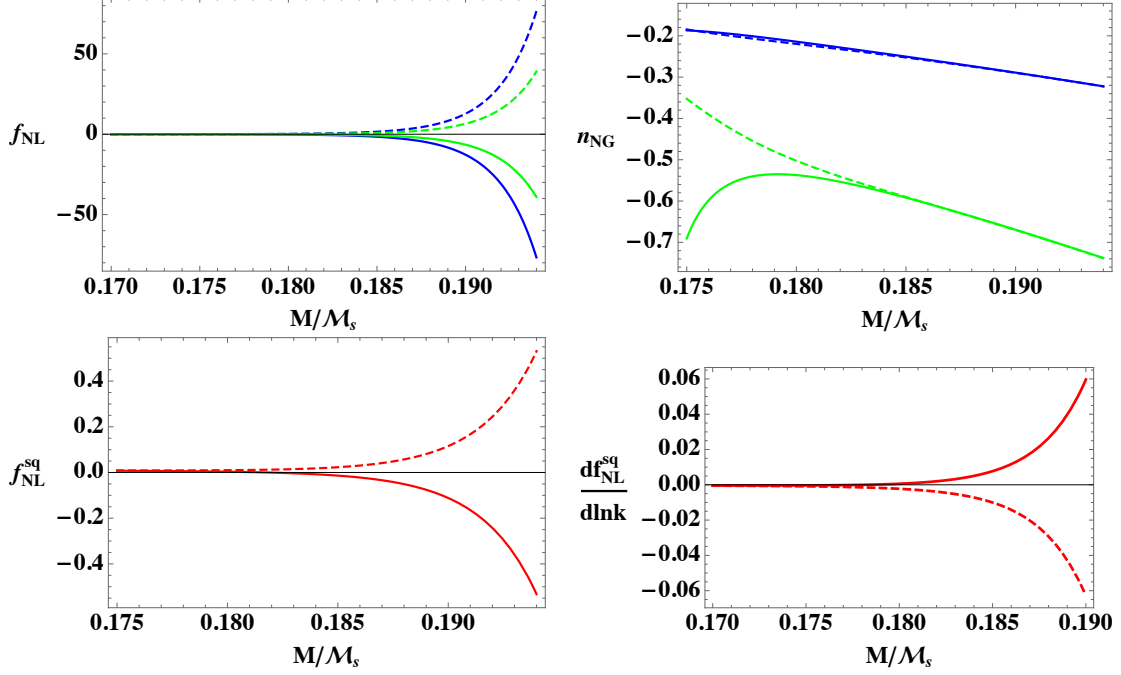


Figure 3. In all of the plots we present various shapes of PNG and their running f_{NL} , $n_{f_{\text{NL}}}$ versus M/M_s for $\lambda_c > 0$ (dashed lines) and $\lambda_c < 0$ (full lines) respectively, while red, blue and green lines represent squeezed, equilateral and orthogonal shapes respectively. For all of these plots we fix the parameters as $\lambda = \pm 4$, $\alpha_1 = 0.4$, $\alpha_{11} = 3.1$, $\alpha_{21} = \alpha_{31} = 1$ and $N = 55$ corresponding to the pivot scale $k_* = a_* H_*$.

6 Distinguishing generalized non-local R^2 -like inflation against EFT of scalar field inflation

In a broader view of developments in inflationary cosmology, we can notice that there are several ways one can construct a viable inflationary phase. Due to the lack of concrete understanding of UV-complete physics, numerous inflationary models were proposed in the past decades [25] taking multiple approaches with different motivations towards UV-completion. In this respect, inflationary cosmology is hugely studied in the context of EFT involving single and multiple scalar fields of different nature [10, 15, 22]. In view of inflationary observables related to 3-point correlations, we shall discuss how to distinguish EFT of several classes of inflationary models against the generalized non-local R^2 -like inflation we have studied in this paper. Note that distinguishing the generalized non-local R^2 -like inflation against the EFT of inflation was extensively discussed in [1].

Canonical single field inflation. This is the simplest framework of understanding inflation driven by a scalar field with the canonical kinetic term and a suitable potential. The successful models of this class are R^2 and Higgs inflation after the conformal transformation to the Einstein frame [8]. Independent of what is the choice of potential, this class of models always satisfy the tensor consistency relation and the Maldacena consistency relation. In our non-local gravity (3.2) these two consistency relations are violated

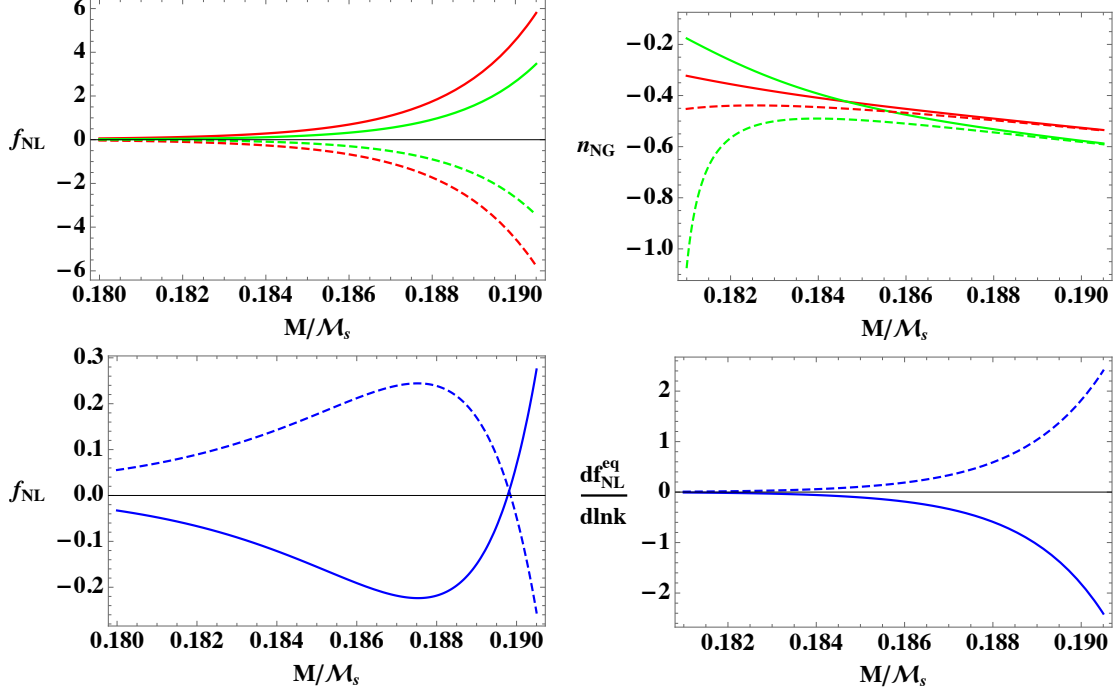


Figure 4. In above plots we present the shapes of PNG and their running f_{NL} , n_{NG} versus M/M_s for $\lambda_c > 0$ (dashed lines) and $\lambda_c < 0$ (full lines) respectively, while red, blue and green lines represent squeezed, equilateral and orthogonal shapes respectively. For all plots we fix the parameters as $\lambda_c = \pm 2$, $\alpha_1 = 0.2$, $\alpha_{11} = 5$, $\alpha_{21} = \alpha_{31} = -1$ and $N = 55$ corresponding to the pivot scale $k_* = a_* H_*$.

(see [1] and our result (4.21)). However, it has been widely understood that such models cannot be really single field ones because any attempt of embedding the models in a UV-complete framework introduce more degrees of freedom which eventually violate the consistency relation (although the new particles which appear in this way could be heavier than the inflaton) [23, 49–51].

Non-canonical single field inflation. Non-canonical scalar field (ϕ) is described by

$$S_{\text{NC}} = \int d^4x \sqrt{-g} \left[\frac{M_p^2}{2} R + P \left(-\frac{1}{2} (\partial\phi)^2, \phi \right) \right] \quad (6.1)$$

where $P(-\frac{1}{2} (\partial\phi)^2, \phi)$ is a generic function of the canonical kinetic term and the field ϕ . This is a general action for a scalar field whose perturbations propagate with a sound speed $0 \leq c_s \leq 1$. Because of this, non-canonical models of inflation can predict a peak in the equilateral shape PNGs, the tensor consistency relation is violated while tensor tilt remains unaffected by c_s :

$$f_{\text{NL}}^{\text{sq}} \sim \frac{1}{c_s^2}, \quad r = 16c_s\epsilon_E, \quad n_t = -2\epsilon_E \quad (6.2)$$

where the slow-roll parameter with subscript ϵ_E denotes the quantity in the canonical scalar field framework of inflation. With the Planck constraints (1.1), we get $c_s \gtrsim 0.02$ [18]. There are two ways we can distinguish our model from a non-canonical scalar one. One way is

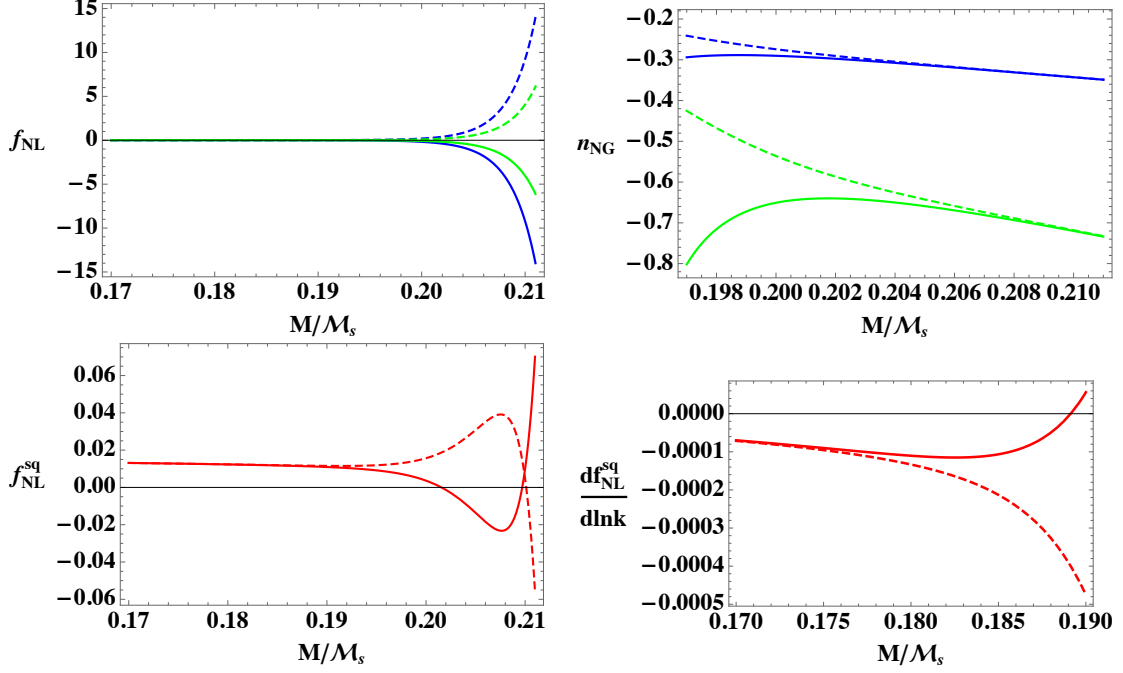


Figure 5. In the above plots we present various shapes of PNG and their running f_{NL} , n_{NG} versus M/M_s . The red, blue and green lines represent squeezed, equilateral and orthogonal shapes respectively. For all these plots we fix the parameters as $\lambda_c = \pm 2$ (-2 for full lines and +2 for dashed lines), $\alpha_1 = 0.2$, $\alpha_{11} = 3.5$, $\alpha_{21} = \alpha_{31} = -1/4$ and $N = 55$ corresponding to the pivot scale $k_* = a_* H_*$.

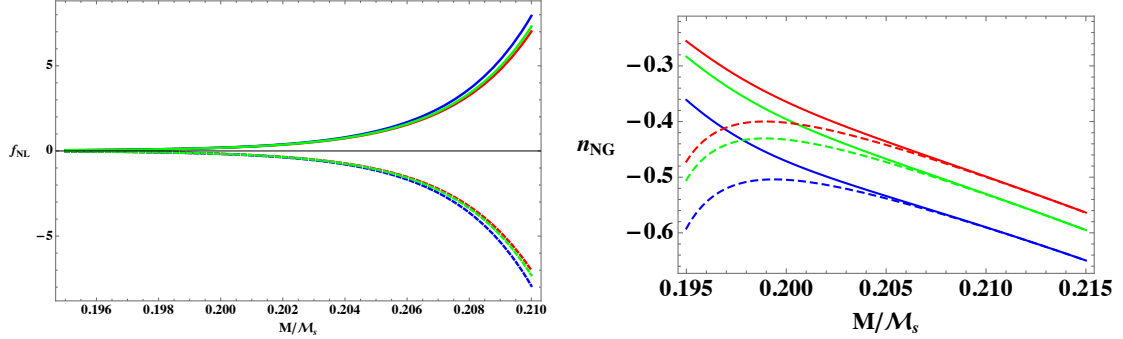


Figure 6. In both plots we present various shapes of PNG and their running f_{NL} , n_{NG} versus M/M_s for $\lambda_c > 0$ (full lines) and $\lambda_c < 0$ (dashed lines) respectively, while red, blue and green lines represent squeezed, equilateral and orthogonal shapes respectively. For both plots we fix the parameters as $\lambda_c = \pm 2$ (+2 corresponding to full lines and -2 represented by lines) $\alpha_1 = 0.2$, $\alpha_{11} = 3$, $\alpha_{21} = -3$, $\alpha_{31} = -1$ and $N = 55$ corresponding to the pivot scale $k_* = a_* H_*$.

that in our case we modify tensor tilt and it becomes scale dependent (see [1]). Another way is provided by the shape of PNGs, in the non-canonical model it is determined by the

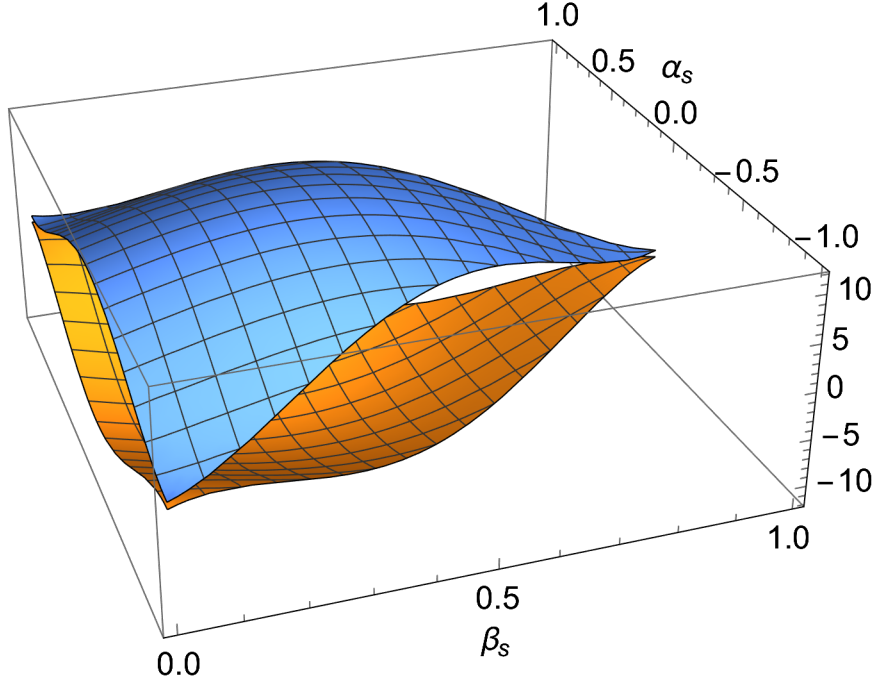


Figure 7. Here we plot $f_{\text{NL}}(1, \alpha_s, \beta_s)$ setting $K = 1$. The values of parameters for this figure are the same as those for the Fig. 3. In this figure, the upper plane in blue shape and lower orange shape represent $\lambda_c > 0$ and $\lambda_c < 0$ respectively.

following interaction terms of curvature perturbation

$$\delta^{(3)}S_{\text{NC}} = \int d^3x d\tau a^2 \left\{ \frac{g_1}{a} \zeta'^3 + g_2 \zeta \zeta'^2 + g_3 \zeta (\partial \zeta)^2 + g_4 \zeta' \partial_j \zeta \partial_j \partial^{-2} \zeta' \right. \\ \left. + g_5 \partial^2 \zeta (\partial_j \partial^{-2} \zeta') (\partial_j \partial^{-2} \zeta') \right\} \quad (6.3)$$

where $\zeta = -\mathcal{R}$ is the curvature perturbation and g_i are functions of slow-roll parameters [46]. If we compare these interaction terms with those we obtained in our theory (4.13), we can deduce that the shapes of PNGs are different, and if the future observations will be powerful enough, we can distinguish our non-local gravity from non-canonical single field models of inflation.

Multifield inflation. Multifield inflation is basically an inflationary scenario driven by multiple scalar fields that leads to curvature and isocurvature perturbations during inflation [52]. Therefore several classes of multifield inflation were studied in literature [30, 53]. Due to the presence of isocurvature modes, curvature perturbation, if defined as being tangent to the background trajectory of inflaton fields in the field space, is generically not time-independent on super-Hubble scales⁶ that leads to violation of the Maldacena consistency relation due to the classical evolution of fluctuations on such scales [52, 56]. As a result

⁶Note, however, that there always exists another mode (a particular solution) of scalar perturbations

of this, the squeezed limit $f_{\text{NL}}^{\text{sq}}$ gives detectable level of non-Gaussianities. In our case we obtain detectable level of $f_{\text{NL}}^{\text{sq}}$ due to the non-local interactions of short and long wavelength modes which are quantum mechanical in nature (See Sec. 4 and Appendix B). Therefore, we generate $f_{\text{NL}}^{\text{sq}}$ in our model in a totally different way compared to multifield inflation. Furthermore, in the context of multifield inflation $f_{\text{NL}}^{\text{sq}}$ is almost scale independent [52]. Moreover, multifield inflation with non-canonical scalar field predicts all three shapes of PNGs (squeezed, equilateral and orthogonal) [29]. In our case we obtain all three shapes in a single field geometric construction of inflation. Particularly, in our case we generate scale dependent PNGs with detectable running (see Sec. 4 and Sec. 5). Furthermore, tensor consistency relation is violated in multifield models of inflation due to the classical evolution of curvature perturbation in the presence of additional isocurvature fields [57]. But this feature can be distinguished from our case because we modify the tensor power spectrum that leads to corrections to the tensor spectral index n_t and its running which are derived in [1].

EFT of single-field inflation.

EFT of single field inflation (EFT-SI) [10, 11] is constructed to unify several single field models of inflation and aims to capture the signatures of UV-completion through the so-called EFT parameters that determine 2-point and 3-point inflationary correlations. It was elaborated in [1] that the physics of two-point correlations in our generalized non-local gravity inflation with (3.2) cannot fall into the category of EFT-SI. The key EFT-SI parameters that affect both 2-point and 3-point correlations are the sound speeds (c_s, c_t) of scalar (curvature) and tensor fluctuations which are slowly varying functions of time. In the EFT model considered in [58], $c_s = 1, c_t \neq 1$ in the original (disformal) frame, while $c_{sE} = \frac{1}{c_t}, c_{tE} = 1$ in the Einstein frame obtained through the disformal transformation which changes the light cone. This leads to relation between scalar and tensor PNGs. In contrast to this, in our case of non-local gravity inflation we have both sounds speeds being unity and the scalar PNGs in our case are determined by the parameter space of the part of our full action (3.2) excluding the terms of the Weyl tensor. Therefore, we do get additional contributions which depend on additional parameter space for tensor PNGs that is the subject of our future investigation [26]. This means that our geometric construction of inflation is indeed clearly distinguishable from that of the EFT-SI [10, 11]. Focusing on the scalar PNGs in particular, the 3rd order action of EFT-SI prescribes

$$\delta_{(s)}^{(3)} S_{\text{EFT-SI}} = \int d^4x \sqrt{-g} \left[\frac{M_p^2}{c_s^2} \epsilon_E \left(\dot{\zeta}^2 - c_s^2 \frac{(\partial_i \zeta)^2}{a^2} \right) - M_p^2 \epsilon_E \left(1 - \frac{1}{c_s^2} \right) \dot{\zeta} \frac{(\partial_i \zeta)^2}{a^2} \right. \\ \left. + \left(\frac{M_p^2}{H} \epsilon_E \left(1 - \frac{1}{c_s^2} \right) + \frac{4}{3} \frac{M_3^4}{H^3} \right) \dot{\zeta}^3 \right]. \quad (6.4)$$

in this case which is (approximately) time-independent in the super-Hubble regime [54, 55] though it is not tangent to the inflaton background trajectory in the field space generically. Its existence can be traced to the fact that the FLRW scale factor is defined up to an arbitrary multiplier in the absence of spatial curvature, see [55] for more discussion.

The above action is derived in the limit then $\epsilon_E \ll c_s^2$ and it contains two interactions $\dot{\zeta}^3$ and $\dot{\zeta}(\partial_i \zeta)^2$ associated with two parameters (c_s, M_3) . These two interactions can be projected into equilateral and orthogonal shapes and the recent Planck data constrained these shapes [18]. Comparing the interactions in (6.4) with our case (4.13), we can easily deduce that non-local gravity does contain more interactions and scale dependencies beyond the standard EFT-SI. Therefore, it would be of great interest to observationally probe (4.13) in the future CMB and LSS observations [32].

EFTs of quasi-single field inflation (aka cosmological collider physics). This is a paradigm where there is one light scalar degree of freedom driving inflation interacting with heavy modes whose mass is of the order of the Hubble scale during inflation [12, 50, 51]. This framework of inflation is a natural set up in several UV-complete theories such as supergravity [23, 59–61]. In this class of inflationary models equilateral, orthogonal and squeezed limit PNGs can be generated due to turns in the inflaton trajectory in the field space (that occur due to the presence of additional heavy fields). The crucial test of quasi-single field inflation is the shape of PNG that is scale dependent in the squeezed limit as follows [62]

$$f_{\text{NL}}^{\text{sq}}(k_{\text{long}}, k_{\text{short}}, k_{\text{short}}) \propto \left(\frac{k_{\text{long}}}{k_{\text{short}}} \right)^{\nu_s} P_{\bar{s}}(\cos \theta) , \quad (6.5)$$

where $P_{\bar{s}}(\cos \theta)$ is the function depending on \bar{s} which is the spin of the heavy particle, θ is the angle between long and short wavelength wave vectors and

$$\nu_s = \frac{3}{2} \pm i \sqrt{\frac{m^2}{H^2} - \frac{9}{4}} \quad (6.6)$$

with m being the mass of the heavy particle. Depending on the mass of the heavy particle, we get different scale dependent features in the shape of PNGs. This is a different scale dependence compared to what we have obtained in (4.21) where f_{NL} has scale dependence on the overall wave number rather than on the short and long wavelength modes in (6.5). This is the distinguishable feature of non-local theories from EFT of quasi-single field inflation.

7 Outlook

In this paper, we have computed and analyzed scalar PNGs which can be generated in the generalized non-local R^2 -like inflation and we provided detailed discussion about how our gravity framework of inflation goes beyond the several EFTs of inflation. Quantitative description of PNG shapes and their running is obtained, too. However, through scalar PNGs we only explored part of the action (3.2) which contributes to f_{NL} in the leading order. It is important to further understand tensor PNGs and cross-correlations that is the subject of our future investigation [26]. Another direction to go forward is to compute 4-point correlations in the generalized non-local gravity inflation and check if the Suyama-Yamaguchi consistency relation [63] gets violated in non-local theories. Furthermore, it is interesting to explore the shapes of PNGs which can emerge if we couple matter degrees of freedom non-minimally and non-locally to gravity [64]. Beyond these studies, it is theoretically very important to study formfactors of our gravity action (3.2) from a more fundamental point of view that can provide us with more robust and precise predictions.

Acknowledgments

AK is supported by FCT Portugal investigator project IF/01607/2015. This research work was supported by grants UID/MAT/00212/2019, COST Action CA15117 (CANTATA). KSK acknowledges the support from JSPS and KAKENHI Grant-in-Aid for Scientific Research No. JP20F20320. AAS was supported by the RSF grant 21-12-00130. We would like to thank L. Buoninfante, A. De Felice, T. Noumi, A. Tokareva, T. Suyama and M. Yamaguchi for very useful discussions.

A Computation of non-Gaussianities

In this section we compute the PNG contributions from the term which is cubic in Ricci scalar in (3.2).

$$\begin{aligned} \delta^{(3)} S_{R^3} = \frac{f_0 \lambda_c}{2\mathcal{M}_s^2} \int d^4x \sqrt{-g} & \left[\mathcal{L}_1(\bar{\square}_s) \delta R \mathcal{L}_2(\bar{\square}_s) \delta R \mathcal{L}_2(\bar{\square}_s) \delta R \right. \\ & \left. + \delta \mathcal{L}_1(\square_s) \bar{R} \delta \mathcal{L}_2(\square_s) \bar{R} \delta \mathcal{L}_3(\square_s) \bar{R} \right] \end{aligned} \quad (\text{A.1})$$

We can notice that (A.1) does not contain any terms involving second variations of Ricci scalar and the 3rd variations of $\sqrt{-g}$ such as

$$\begin{aligned} & \bullet \mathcal{L}_i(\square_s) \delta^{(2)} R \mathcal{L}_j(\square_s) \bar{R} \mathcal{L}_k(\square_s) \delta R \\ & \bullet \mathcal{L}_i(\square_s) \delta^{(2)} R \mathcal{L}_j(\square_s) \bar{R} \mathcal{L}_k(\square_s) \delta \bar{R} \\ & \bullet \delta^{(2)} \sqrt{-g} \mathcal{L}_i(\square_s) \bar{R} \mathcal{L}_j(\square_s) \bar{R} \mathcal{L}_k(\square_s) \bar{R} \end{aligned} \quad (\text{A.2})$$

since any such terms be multiplied by $\mathcal{L}_i(\bar{\square}_s) \bar{R}$ which become zero after imposing the on-shell condition (3.6). Further simplifying (A.1) using the following formula [27]

$$\delta \mathcal{L}_i(\square_s) = \sum_n L_{in} \sum_{a+b=n-1} \bar{\square}_s^a \delta \square_s \bar{\square}_s^b, \quad (\text{A.3})$$

we obtain

$$\begin{aligned} \delta_{(s)}^{(3)} S_{R+R^2}^{\text{Non-local}} &= \delta^{(3)} S_{R+R^2}^{\text{local}} + \frac{f_0 \lambda_c}{2\mathcal{M}_s^2} \int d^4x \sqrt{-g} \left[\left(\mathcal{L}_1(\bar{\square}_s) \delta R + \frac{\mathcal{L}_1(\bar{\square}_s)}{\bar{\square}_s - \frac{M^2}{\mathcal{M}_s^2}} \delta \square_s \bar{R} \right) \right. \\ & \quad \left(\mathcal{L}_2(\bar{\square}_s) \delta R + \frac{\mathcal{L}_2(\bar{\square}_s)}{\bar{\square}_s - \frac{M^2}{\mathcal{M}_s^2}} \delta \square_s \bar{R} \right) \left(\mathcal{L}_3(\bar{\square}_s) \delta R + \frac{\mathcal{L}_3(\bar{\square}_s)}{\bar{\square}_s - \frac{M^2}{\mathcal{M}_s^2}} \delta \square_s \bar{R} \right) \Big] \\ &= \delta^{(3)} S_{R+R^2}^{\text{local}} - \frac{f_0 \lambda_c \epsilon^3}{2\mathcal{M}_s^2} \int d^4x \sqrt{-g} \left\{ \left[\frac{64}{a^6} \mathcal{H}^3 \left(8\epsilon^3 T_{\text{NL}}^4 + 4\epsilon^2 T_{\text{NL}}^3 \right. \right. \right. \\ & \quad \left. \left. \left. 2\epsilon T_{\text{NL}}^2 + T_{\text{NL}}^1 \right) \mathcal{R}' \mathcal{R}' \mathcal{R}' + \frac{64}{a^2} \bar{R}_{\text{dS}} \mathcal{H}^2 (4\epsilon^2 T_{\text{NL}}^3 + 2\epsilon T_{\text{NL}}^2 + T_{\text{NL}}^1) \mathcal{R} \mathcal{R}' \mathcal{R}' \right. \right. \\ & \quad \left. \left. \left. \frac{128}{a^2} \bar{R}_{\text{dS}}^2 \mathcal{H} (\epsilon T_{\text{NL}}^2 + T_{\text{NL}}^1) \mathcal{R} \mathcal{R} \mathcal{R}' + 64 \bar{R}_{\text{dS}}^3 T_{\text{NL}}^1 \mathcal{R}^3 \right] \right\}. \end{aligned} \quad (\text{A.4})$$

where $\mathcal{H} = aH$ is the Hubble factor in conformal time. Here we have used the slow-roll approximation in the next to leading order in ϵ and made a substitution $\bar{\square}_{\text{dS}}\mathcal{R} = M^2\mathcal{R}$ which solution in the quasi-dS approximation is

$$\mathcal{R} \approx -\frac{1}{2\epsilon} \frac{1}{\sqrt{3f_0\bar{R}_{\text{dS}}}} \frac{H}{\sqrt{2k^3}} (1 + ik\tau) e^{-ik\tau}. \quad (\text{A.5})$$

This follows from the computations in [1]. We have also used the following relations which were derived using quasi-dS approximation (see Eqs (B.5) and (B.7) in [27]):

$$\begin{aligned} \mathcal{O}(\bar{\square}_s) \delta R &\approx \mathcal{O}\left(\frac{2M^2}{\mathcal{M}_s^2}\right) 2\bar{R}\Psi + \frac{2\bar{R}}{M^2} H\epsilon \left[\mathcal{O}\left(\frac{2M^2}{\mathcal{M}_s^2}\right) - \mathcal{O}(0) \right] \dot{\Psi} \\ &\quad + 16H\epsilon \left[\mathcal{O}\left(\frac{M^2}{\mathcal{M}_s^2} + \frac{\bar{R}}{4\mathcal{M}_s^2}\right) - \mathcal{O}(0) \right] \dot{\Psi} \\ \mathcal{O}(\square_s) \delta \square_s \bar{R} &\approx \frac{2M^2}{\mathcal{M}_s^2} \mathcal{O}\left(\frac{2M^2}{\mathcal{M}_s^2}\right) \bar{R}\Psi - \frac{2\bar{R}H\epsilon}{\mathcal{M}_s^2} \mathcal{O}\left(\frac{M^2}{\mathcal{M}_s^2} + \frac{\bar{R}}{4\mathcal{M}_s^2}\right) \dot{\Psi} \end{aligned} \quad (\text{A.6})$$

where \mathcal{O} denotes an analytic function of d'Alembertian \square . In (A.4) we carefully kept all terms up to the leading order in $\epsilon \approx \frac{1}{2N}$ and neglected higher order contributions of $\mathcal{O}\left(\frac{1}{N^2}\right)$ treating $\epsilon \approx \text{const}$. In our computation we re-sum contribution of all the infinite derivative terms. In the second line of (A.4), we made simplifications using (4.19). Since our case is single field inflation, perturbed modes deep inside the Hubble radius during inflation are evaluated at the Hubble radius exit since curvature perturbations remains constant on super-Hubble scales $k \ll aH$. So the 3-point correlations of \mathcal{R} do not evolve after that. Therefore, we evaluate the 3-point correlations at the moment when $\tau_e \sim -\frac{1}{k}$ which is a conformal time after few e-foldings of the Hubble radius exit [45].

Here

$$\begin{aligned} \mathcal{T}_{\text{NL}} &= \mathcal{F}_R \left(\frac{M^2}{\mathcal{M}_s^2} + \frac{\bar{R}_{\text{dS}}}{4\mathcal{M}_s^2} \right) - \mathcal{F}_1 \approx \mathcal{F}_R \left(\frac{\bar{R}_{\text{dS}}}{4\mathcal{M}_s^2} \right) - \mathcal{F}_1 + \epsilon \frac{\bar{R}_{\text{dS}}}{8\mathcal{M}_s^2} \mathcal{F}_R^{(\dagger)} \left(\frac{\bar{R}_{\text{dS}}}{4\mathcal{M}_s^2} \right). \quad (\text{A.7}) \\ T_{\text{NL}}^1 &= \sum_{i,j,k,i \neq j \neq k} \mathcal{L}_i \left(\frac{2M^2}{\mathcal{M}_s^2} \right) \mathcal{L}_j \left(\frac{2M^2}{\mathcal{M}_s^2} \right) \mathcal{L}_k \left(\frac{2M^2}{\mathcal{M}_s^2} \right), \\ T_{\text{NL}}^2 &= \sum_{i,j,k,i \neq j \neq k} \mathcal{L}_i \left(\frac{2M^2}{\mathcal{M}_s^2} \right) \mathcal{L}_j \left(\frac{2M^2}{\mathcal{M}_s^2} \right) \mathcal{L}_k \left(\frac{M^2}{\mathcal{M}_s^2} + \frac{\bar{R}_{\text{dS}}}{4\mathcal{M}_s^2} \right), \\ T_{\text{NL}}^3 &= \sum_{i,j,k,i \neq j \neq k} \mathcal{L}_i \left(\frac{2M^2}{\mathcal{M}_s^2} \right) \mathcal{L}_j \left(\frac{M^2}{\mathcal{M}_s^2} + \frac{\bar{R}_{\text{dS}}}{4\mathcal{M}_s^2} \right) \mathcal{L}_k \left(\frac{M^2}{\mathcal{M}_s^2} + \frac{\bar{R}_{\text{dS}}}{4\mathcal{M}_s^2} \right), \\ T_{\text{NL}}^4 &= \sum_{i,j,k,i \neq j \neq k} \mathcal{L}_i \left(\frac{M^2}{\mathcal{M}_s^2} + \frac{\bar{R}_{\text{dS}}}{4\mathcal{M}_s^2} \right) \mathcal{L}_j \left(\frac{M^2}{\mathcal{M}_s^2} + \frac{\bar{R}_{\text{dS}}}{4\mathcal{M}_s^2} \right) \mathcal{L}_k \left(\frac{M^2}{\mathcal{M}_s^2} + \frac{\bar{R}_{\text{dS}}}{4\mathcal{M}_s^2} \right). \end{aligned} \quad (\text{A.8})$$

Considering the formfactors of the form (3.5) with the conditions imposed in (3.6), we can easily deduce that

$$T_{\text{NL}}^1 \ll T_{\text{NL}}^2 \ll T_{\text{NL}}^3 \ll T_{\text{NL}}^4 \quad (\text{A.9})$$

in the limit of $M^2 \ll \mathcal{M}_s^2$ and $\bar{R}_{\text{dS}} \gtrsim \mathcal{M}_s^2$. Note that since T_{NL}^1 does not depend on the ratio $\frac{\bar{R}_{\text{dS}}}{\mathcal{M}_s^2}$, we found its contributions are far less than the contributions involving $T_{\text{NL}}^2 - T_{\text{NL}}^4$, especially for the operators $\ell_i(\square_s)$ of the form in (3.7).

B On violation of Maldacena consistency relation in non-local gravity

The goal of this section is to illustrate how the Maldacena consistency relation can be easily violated in non-local gravity. We provide here an explicit illustrative example from our study carried in this paper. It has been argued that the Maldacena consistency relation given by [37, 48, 65]

$$f_{\text{NL}}^{\text{sq}} = \frac{5}{12} (1 - n_s) \quad (\text{B.1})$$

cannot be violated in any single field slow-roll inflation with adiabatic vacuum initial conditions. The above relation was intuitively argued to be valid as follows. Since the curvature perturbation is constant on super-Hubble scales, the perturbed metric (say with wave-number k_1) in the so-called unitary gauge in which the inflaton perturbations can be put to zero [48, 65] is approximated to be ⁷

$$ds^2 = -dt^2 + e^{2\zeta_{k_1}} a^2(t) dx^2, \quad (\text{B.2})$$

where the part of the scalar perturbations related to lapse \mathcal{N} and shift functions \mathcal{N}_i in the well-known Arnowitt-Deser-Misner (ADM) formalism [37] are approximated to zero as they depend on the time and spatial derivatives of ζ which is constant on the super-Hubble scales. Therefore, according to the standard intuitive proof [48, 65] that is well supported by EFT of single-field inflation, the 3-point correlation in the squeezed limit $k_1 \ll k_2 = k_3 = k$ can be decomposed as (using the simple Taylor expansion of 2-point correlation of short wavelength mode in the effective background metric (B.2))

$$\begin{aligned} \lim_{k_1 \rightarrow 0} \langle \zeta_{\mathbf{k}_1} \zeta_{\mathbf{k}_2} \zeta_{\mathbf{k}_3} \rangle &\approx \lim_{k_1 \rightarrow 0} \langle \zeta_{\mathbf{k}_1} \langle \zeta_{\mathbf{k}_2} \zeta_{\mathbf{k}_3} \rangle \rangle \\ &= -(2\pi)^3 \delta^3 \left(\sum_i \mathbf{k}_i \right) (n_s - 1) P_{k_1} P_{k_3} \end{aligned} \quad (\text{B.3})$$

where P_{k_1}, P_{k_3} are the power spectrum of k_1 mode and k_3 mode respectively. In deriving the above result, the trick of rescaling the spatial coordinates $x^i \rightarrow e^{\zeta_{k_1}} x^i$ is used since ζ_{k_1} can be treated as a constant on super-Hubble scales that was shown in [55, 65, 66]. The above result is also concretely established and proved in local scalar-tensor theories.

In the context of non-local gravity we have seen that non-local interactions of curvature perturbations evade the above result (as we can witness from the expression of $f_{\text{NL}}^{\text{eq}}$ in (4.21)). To illustrate this, we consider a part of the action (3.2) with local $R + R^2$ terms and the non-local cubic scalar curvature term

$$S_{R+R^2+R^3}^{\text{Non-local}} = S_{R+R^2}^{\text{local}} + S_{R^3}^{\text{Non-local}} \quad (\text{B.4})$$

where $S_{R+R^2}^{\text{local}}, S_{R^3}^{\text{Non-local}}$ are defined in (4.8) with condition (3.6).

⁷C.f. Eq. (17) in [66] where $t_0(\mathbf{r})$ is just $\frac{\zeta(\mathbf{r})}{H}$ up to a constant, and $|\zeta|$ need not be small. In that paper, the synchronous gauge with additional conditions excluding two gauge modes was used but the resulting form of the metric in the leading approximation for $t \gg t_0$ appeared to be essentially the same as (B.2).

Computing the second order perturbed action of (B.4) around the FLRW background obtained from (3.1), we can deduce that

$$\delta^{(2)} S_{R+R^2+R^3}^{\text{Non-local}} = \delta^{(2)} S_{R+R^2}^{\text{local}}, \quad (\text{B.5})$$

where $\delta^{(2)} S_{R^3}^{\text{Non-local}} \Big|_{\bar{\square}=M^2 \bar{R}} = 0$ which is the result derived in [1]. This means that at the second order perturbation level, (B.4) is exactly equivalent to local R^2 inflation and we can easily confirm that curvature perturbation is conserved on super-Hubble scales. But if we go to the interaction level, that is when we compute the bi-spectrum, we generate non-trivial contributions from the non-local interactions generated from the non-local cubic in scalar curvature term. These new contributions violate the Maldacena consistency relation as we can see from expression (4.21). Therefore, we can now precisely deduce that (B.4) is a counterexample to the intuitive derivation of the Maldacena consistency relation (B.3) because in the case of inflation with (B.4) we can see from the second order action that it is single field and slow-roll inflation since the background solutions is (3.1), but still we do violate the Maldacena consistency relation. This happens because the relations (4.19) lead to the enhancement of the interaction strength between the long wavelength mode and short wavelength modes beyond this order of slow-roll since $\bar{R} \gtrsim \mathcal{M}_s^2$.

So in summary, the proof (B.3) can only be valid in local theories, in particular two derivative theories, where the perturbed metric can be approximated as (B.2). Then one can Taylor expand 3-point correlation in the squeezed limit. In the case of non-local theory, one cannot apply this simple Taylor expansion because vertices come with formfactors of infinite derivative structure which we localize the action using the on-shell relations (4.19). This alters significantly the interaction picture and we get an exponential enhancement of 3-point vertices due to the structure of formfactors (3.4). However, we are well within the perturbative regime because the non-linear corrections to curvature perturbation in non-local R^2 -like inflation are still small and fluctuations are indeed very Gaussian as the current data suggest [18].

References

- [1] A. S. Koshelev, K. S. Kumar, and A. A. Starobinsky, “Generalized non-local R^2 -like inflation,” [arXiv:2209.02515 \[hep-th\]](#).
- [2] A. A. Starobinsky, “A New Type of Isotropic Cosmological Models Without Singularity,” *Phys. Lett. B* **91** (1980) 99–102.
- [3] A. A. Starobinsky, “Nonsingular Model of the Universe with the Quantum Gravitational De Sitter Stage and its Observational Consequences,” in *Proc. of the Second Seminar “Quantum Theory of Gravity”, Moscow Oct. 1981, INR Press, Moscow (1982)*, pp. 58–72.
- [4] A. A. Starobinsky, “The Perturbation Spectrum Evolving from a Nonsingular Initially De-Sitter Cosmology and the Microwave Background Anisotropy,” *Sov. Astron. Lett.* **9** (1983) 302–304.
- [5] A. Vilenkin, “Classical and Quantum Cosmology of the Starobinsky Inflationary Model,” *Phys. Rev. D* **32** (1985) 2511.

- [6] M. B. Mijic, M. S. Morris, and W.-M. Suen, “The R^2 Cosmology: Inflation Without a Phase Transition,” *Phys. Rev. D* **34** (1986) 2934.
- [7] K.-i. Maeda, “Inflation as a Transient Attractor in R^2 Cosmology,” *Phys. Rev. D* **37** (1988) 858.
- [8] **Planck** Collaboration, Y. Akrami *et al.*, “Planck 2018 results. X. Constraints on inflation,” [arXiv:1807.06211](#) [[astro-ph.CO](#)].
- [9] **BICEP, Keck** Collaboration, P. A. R. Ade *et al.*, “Improved Constraints on Primordial Gravitational Waves using Planck, WMAP, and BICEP/Keck Observations through the 2018 Observing Season,” *Phys. Rev. Lett.* **127** no. 15, (2021) 151301, [arXiv:2110.00483](#) [[astro-ph.CO](#)].
- [10] C. Cheung, P. Creminelli, A. L. Fitzpatrick, J. Kaplan, and L. Senatore, “The Effective Field Theory of Inflation,” *JHEP* **03** (2008) 014, [arXiv:0709.0293](#) [[hep-th](#)].
- [11] S. Weinberg, “Effective Field Theory for Inflation,” *Phys. Rev. D* **77** (2008) 123541, [arXiv:0804.4291](#) [[hep-th](#)].
- [12] X. Chen, “Primordial Non-Gaussianities from Inflation Models,” *Adv. Astron.* **2010** (2010) 638979, [arXiv:1002.1416](#) [[astro-ph.CO](#)].
- [13] Z. Kenton and D. J. Mulryne, “The squeezed limit of the bispectrum in multi-field inflation,” *JCAP* **10** (2015) 018, [arXiv:1507.08629](#) [[astro-ph.CO](#)].
- [14] **Planck** Collaboration, Y. Akrami *et al.*, “Planck 2018 results. IX. Constraints on primordial non-Gaussianity,” *Astron. Astrophys.* **641** (2020) A9, [arXiv:1905.05697](#) [[astro-ph.CO](#)].
- [15] T. Kobayashi, M. Yamaguchi, and J. Yokoyama, “Generalized G-inflation: Inflation with the most general second-order field equations,” *Prog. Theor. Phys.* **126** (2011) 511–529, [arXiv:1105.5723](#) [[hep-th](#)].
- [16] E. Komatsu and et al, “Non-Gaussianity as a Probe of the Physics of the Primordial Universe and the Astrophysics of the Low Redshift Universe,” *Science White Paper submitted to the Cosmology and Fundamental Physics (CFP) Science Frontier Panel of the Astro 2010 Decadal Survey* (2009) , [arXiv:0902.4759](#).
- [17] S. Bahrami and E. E. Flanagan, “Primordial non-Gaussianities in single field inflationary models with non-trivial initial states,” *JCAP* **10** (2014) 010, [arXiv:1310.4482](#) [[astro-ph.CO](#)].
- [18] **Planck** Collaboration, Y. Akrami *et al.*, “Planck 2018 results. IX. Constraints on primordial non-Gaussianity,” [arXiv:1905.05697](#) [[astro-ph.CO](#)].
- [19] X. Chen, M.-x. Huang, S. Kachru, and G. Shiu, “Observational signatures and non-Gaussianities of general single field inflation,” *JCAP* **0701** (2007) 002, [arXiv:hep-th/0605045](#) [[hep-th](#)].
- [20] X. Chen, “Running non-Gaussianities in DBI inflation,” *Phys. Rev. D* **72** (2005) 123518, [arXiv:astro-ph/0507053](#).
- [21] P. Creminelli, G. D’Amico, M. Musso, J. Norena, and E. Trincherini, “Galilean symmetry in the effective theory of inflation: new shapes of non-Gaussianity,” *JCAP* **02** (2011) 006, [arXiv:1011.3004](#) [[hep-th](#)].
- [22] L. Senatore and M. Zaldarriaga, “The Effective Field Theory of Multifield Inflation,” *JHEP* **04** (2012) 024, [arXiv:1009.2093](#) [[hep-th](#)].

- [23] N. Arkani-Hamed and J. Maldacena, “Cosmological Collider Physics,” [arXiv:1503.08043 \[hep-th\]](#).
- [24] X. Chen and Y. Wang, “Quasi-Single Field Inflation and Non-Gaussianities,” *JCAP* **1004** (2010) 027, [arXiv:0911.3380 \[hep-th\]](#).
- [25] J. Martin, C. Ringeval, and V. Vennin, “Encyclopædia Inflationaris,” *Phys. Dark Univ.* **5-6** (2014) 75–235, [arXiv:1303.3787 \[astro-ph.CO\]](#).
- [26] A. S. Koshelev, K. Sravan Kumar, and A. A. Starobinsky, “Generalized R^2 -like inflation and tensor non-Gaussianities,” [arXiv:2211.XXXX \[hep-th\]](#).
- [27] A. S. Koshelev, K. Sravan Kumar, A. Mazumdar, and A. A. Starobinsky, “Non-Gaussianities and tensor-to-scalar ratio in non-local R^2 -like inflation,” *JHEP* **06** (2020) 152, [arXiv:2003.00629 \[hep-th\]](#).
- [28] **Planck** Collaboration, P. A. R. Ade *et al.*, “Planck 2015 results. XVII. Constraints on primordial non-Gaussianity,” *Astron. Astrophys.* **594** (2016) A17, [arXiv:1502.01592 \[astro-ph.CO\]](#).
- [29] X. Gao, “Primordial Non-Gaussianities of General Multiple Field Inflation,” *JCAP* **0806** (2008) 029, [arXiv:0804.1055 \[astro-ph\]](#).
- [30] C. T. Byrnes, “Lecture notes on non-Gaussianity,” *Astrophys. Space Sci. Proc.* **45** (2016) 135–165, [arXiv:1411.7002 \[astro-ph.CO\]](#).
- [31] F. Oppizzi, M. Liguori, A. Renzi, F. Arroja, and N. Bartolo, “CMB constraints on running non-Gaussianity,” *JCAP* **05** (2018) 045, [arXiv:1711.08286 \[astro-ph.CO\]](#).
- [32] P. D. Meerburg *et al.*, “Primordial Non-Gaussianity,” [arXiv:1903.04409 \[astro-ph.CO\]](#).
- [33] D. Karagiannis, A. Lazanu, M. Liguori, A. Raccanelli, N. Bartolo, and L. Verde, “Constraining primordial non-Gaussianity with bispectrum and power spectrum from upcoming optical and radio surveys,” *Mon. Not. Roy. Astron. Soc.* **478** no. 1, (2018) 1341–1376, [arXiv:1801.09280 \[astro-ph.CO\]](#).
- [34] E. Castorina, Y. Feng, U. Seljak, and F. Villaescusa-Navarro, “Primordial non-Gaussianities and zero bias tracers of the Large Scale Structure,” *Phys. Rev. Lett.* **121** no. 10, (2018) 101301, [arXiv:1803.11539 \[astro-ph.CO\]](#).
- [35] J. B. Muñoz, Y. Ali-Haïmoud, and M. Kamionkowski, “Primordial non-gaussianity from the bispectrum of 21-cm fluctuations in the dark ages,” *Phys. Rev. D* **92** no. 8, (2015) 083508, [arXiv:1506.04152 \[astro-ph.CO\]](#).
- [36] T. Flöss, T. de Wild, P. D. Meerburg, and L. V. E. Koopmans, “The Dark Ages’ 21-cm Trispectrum,” [arXiv:2201.08843 \[astro-ph.CO\]](#).
- [37] J. M. Maldacena, “Non-Gaussian features of primordial fluctuations in single field inflationary models,” *JHEP* **05** (2003) 013, [arXiv:astro-ph/0210603 \[astro-ph\]](#).
- [38] A. De Felice and S. Tsujikawa, “Primordial non-Gaussianities in general modified gravitational models of inflation,” *JCAP* **1104** (2011) 029, [arXiv:1103.1172 \[astro-ph.CO\]](#).
- [39] E. Komatsu and D. N. Spergel, “Acoustic signatures in the primary microwave background bispectrum,” *Phys. Rev. D* **63** (2001) 063002, [arXiv:astro-ph/0005036 \[astro-ph\]](#).
- [40] T. Takahashi, “Primordial non-Gaussianity and the inflationary Universe,” *PTEP* **2014** no. 6, (2014) 06B105.

- [41] K. Sravan Kumar, S. Maheshwari, and A. Mazumdar, “Perturbations in higher derivative gravity beyond maximally symmetric spacetimes,” *Phys. Rev. D* **100** no. 6, (2019) 064022, [arXiv:1905.03227 \[gr-qc\]](#).
- [42] J. R. Fergusson and E. P. S. Shellard, “The shape of primordial non-Gaussianity and the CMB bispectrum,” *Phys. Rev. D* **80** (2009) 043510, [arXiv:0812.3413 \[astro-ph\]](#).
- [43] D. Babich, P. Creminelli, and M. Zaldarriaga, “The Shape of non-Gaussianities,” *JCAP* **0408** (2004) 009, [arXiv:astro-ph/0405356 \[astro-ph\]](#).
- [44] D. Seery, “Infrared effects in inflationary correlation functions,” *Class. Quant. Grav.* **27** (2010) 124005, [arXiv:1005.1649 \[astro-ph.CO\]](#).
- [45] E. Pajer, G. L. Pimentel, and J. V. S. Van Wijck, “The Conformal Limit of Inflation in the Era of CMB Polarimetry,” *JCAP* **1706** no. 06, (2017) 009, [arXiv:1609.06993 \[hep-th\]](#).
- [46] C. Burrage, R. H. Ribeiro, and D. Seery, “Large slow-roll corrections to the bispectrum of noncanonical inflation,” *JCAP* **07** (2011) 032, [arXiv:1103.4126 \[astro-ph.CO\]](#).
- [47] A. De Felice and S. Tsujikawa, “f(R) theories,” *Living Rev. Rel.* **13** (2010) 3, [arXiv:1002.4928 \[gr-qc\]](#).
- [48] P. Creminelli and M. Zaldarriaga, “Single field consistency relation for the 3-point function,” *JCAP* **10** (2004) 006, [arXiv:astro-ph/0407059](#).
- [49] A. Linde, “Inflationary Cosmology after Planck 2013,” in *Proceedings, 100th Les Houches Summer School: Post-Planck Cosmology: Les Houches, France, July 8 - August 2, 2013*, pp. 231–316. 2015. [arXiv:1402.0526 \[hep-th\]](#).
<https://inspirehep.net/record/1280019/files/arXiv:1402.0526.pdf>.
- [50] T. Noumi, M. Yamaguchi, and D. Yokoyama, “Effective field theory approach to quasi-single field inflation and effects of heavy fields,” *JHEP* **06** (2013) 051, [arXiv:1211.1624 \[hep-th\]](#).
- [51] H. Lee, D. Baumann, and G. L. Pimentel, “Non-Gaussianity as a Particle Detector,” *JHEP* **12** (2016) 040, [arXiv:1607.03735 \[hep-th\]](#).
- [52] D. Wands, “Multiple field inflation,” *Lect. Notes Phys.* **738** (2008) 275–304, [arXiv:astro-ph/0702187](#).
- [53] V. Vennin, K. Koyama, and D. Wands, “Encyclopædia curvatonis,” *JCAP* **11** (2015) 008, [arXiv:1507.07575 \[astro-ph.CO\]](#).
- [54] A. A. Starobinsky and J. Yokoyama, “Density fluctuations in Brans-Dicke inflation,” in *Proc. of 4th Workshop on General Relativity and Gravitation*, eds. K. Nakao et al. (Kyoto University, 1995), pp. 381–390. [arXiv:gr-qc/9502002](#).
- [55] A. A. Starobinsky, S. Tsujikawa, and J. Yokoyama, “Cosmological perturbations from multifield inflation in generalized Einstein theories,” *Nucl. Phys. B* **610** (2001) 383–410, [arXiv:astro-ph/0107555](#).
- [56] F. Vernizzi and D. Wands, “Non-gaussianities in two-field inflation,” *JCAP* **05** (2006) 019, [arXiv:astro-ph/0603799](#).
- [57] D. Polarski and A. A. Starobinsky, “Structure of primordial gravitational waves spectrum in a double inflationary model,” *Phys. Lett. B* **356** (1995) 196–204, [arXiv:astro-ph/9505125](#).
- [58] P. Creminelli, J. Gleyzes, J. Noreña, and F. Vernizzi, “Resilience of the standard predictions for primordial tensor modes,” *Phys. Rev. Lett.* **113** no. 23, (2014) 231301, [arXiv:1407.8439 \[astro-ph.CO\]](#).

- [59] N. Bartolo, D. M. Bianco, R. Jimenez, S. Matarrese, and L. Verde, “Supergravity, α -attractors and primordial non-Gaussianity,” *JCAP* **10** (2018) 017, [arXiv:1805.04269 \[astro-ph.CO\]](#).
- [60] A. Hetz and G. A. Palma, “Sound Speed of Primordial Fluctuations in Supergravity Inflation,” *Phys. Rev. Lett.* **117** no. 10, (2016) 101301, [arXiv:1601.05457 \[hep-th\]](#).
- [61] S. Aoki and M. Yamaguchi, “Disentangling mass spectra of multiple fields in cosmological collider,” *JHEP* **04** (2021) 127, [arXiv:2012.13667 \[hep-th\]](#).
- [62] X. Chen, M. H. Namjoo, and Y. Wang, “Quantum Primordial Standard Clocks,” *JCAP* **02** (2016) 013, [arXiv:1509.03930 \[astro-ph.CO\]](#).
- [63] T. Suyama and M. Yamaguchi, “Non-Gaussianity in the modulated reheating scenario,” *Phys. Rev. D* **77** (2008) 023505, [arXiv:0709.2545 \[astro-ph\]](#).
- [64] T. Draper, B. Knorr, C. Ripken, and F. Saueressig, “Graviton-Mediated Scattering Amplitudes from the Quantum Effective Action,” *JHEP* **11** (2020) 136, [arXiv:2007.04396 \[hep-th\]](#).
- [65] P. Creminelli, G. D’Amico, M. Musso, and J. Norena, “The (not so) squeezed limit of the primordial 3-point function,” *JCAP* **11** (2011) 038, [arXiv:1106.1462 \[astro-ph.CO\]](#).
- [66] A. A. Starobinsky, “Dynamics of Phase Transition in the New Inflationary Universe Scenario and Generation of Perturbations,” *Phys. Lett. B* **117** (1982) 175–178.